

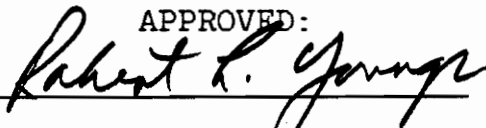
RELATIONSHIP OF BACTERIAL INFECTION
AND STRESS WAVE TRAVEL TIME
IN RED OAK LUMBER

by

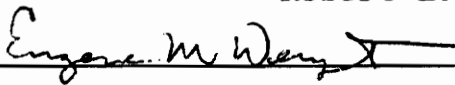
Erkki I. Verkasalo

Thesis submitted to the Faculty of the
Virginia Polytechnic Institute and State University
in partial fulfillment of the requirements
for the degree of
MASTER OF SCIENCE
in
Forestry and Forest Products

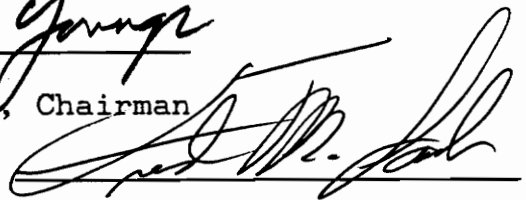
APPROVED:



Robert L. Youngs, Chairman



Eugene M. Wengert



Fred M. Lamb

December, 1991

Blacksburg, Virginia

c.2

LD
5655
V855
1991
V474
c.2

RELATIONSHIP OF BACTERIAL INFECTION
AND STRESS WAVE TRAVEL TIME
IN RED OAK LUMBER

by

Erkki I. Verkasalo

Robert L. Youngs, Chairman

Wood Science and Forest Products

(ABSTRACT)

Anaerobic bacterial infection increases the proclivity of red oak lumber to develop surface, internal and end checks, and develop or aggravate ring failure during drying. It also extends the drying time. Bacterial infection is hard to identify before drying without the use of costly, time-consuming tests. Thus, there is a need for an inexpensive, rapid and accurate method for the identification that can be used at a mill.

This research project investigated the possibility to use stress wave timing for the identification of bacterial infection, by studying the relationship of the level of bacterial infection and impact-induced stress wave travel time across the grain of green 4/4 red oak lumber from

Southcentral Virginia. Bacterial infection increased stress wave travel time, but a considerable overlap existed between infected and uninfected boards.

Tests on tensile strength perpendicular to grain, which is critical for lumber to check during drying showed a decrease in strength due to the bacterial infection. A parallel kiln-drying experiment, following a standard drying schedule (T4D2), showed more drying defects in the infected lumber than in the uninfected lumber. Defects were also more frequent in lumber with a long stress wave travel time than in lumber with a short stress wave travel time.

ACKNOWLEDGEMENTS

I would like to express my best gratitude to my advisor, Dr. Robert Youngs, for his patience, support, and constant guidance from the start to the completion of this project. The members of my committee, Dr. Eugene Wengert and Dr. Fred Lamb, my instructors at the U.S. Forest Products Laboratory, Project Leader Antoni TenWolde, Dr. Robert Ross, and Dr. James Ward, and Manager Holt Hogan from Ontario Hardwood Co., Inc., Ontario, Virginia also strongly contributed to the completion with their help and advice.

TABLE OF CONTENTS

	Page
1. INTRODUCTION	1
2. HYPOTHESES	3
3. OBJECTIVES	4
4. LITERATURE REVIEW	5
41. Bacterial Infection in Red Oak Wood	5
411. Occurrence and Causes	5
412. Related Problems	7
4121. Shake and Frost Cracks	7
4122. Reduced Strength of Wood	8
4123. Drying Degrade	8
42. Stress Wave Nondestructive Evaluation of Wood	11
421. Concepts and Fundamental Theories	11
422. Verifications and Applications	13
4221. Sound Wood	13
4222. Bacterially Infected Wood	15
5. EXPERIMENTAL PROCEDURES	17
51. Procurement of Material	17
511. Logs and Lumber at the Saw Mill	17
512. Lumber Handling at the U.S. Forest Products Laboratory	19
52. Data Collection Details	20

521. Establishing the Presence of Bacterial Infection	20
522. Verifying the Presence of Bacterial Infection	24
523. Measurement of Moisture Content and Density	32
524. Stress Wave Analysis	35
525. Tensile Strength Tests Perpendicular to Grain	40
526. Kiln-Drying Experiment	44
527. Evaluation of Drying Defects	47
53. Data Analysis	49
531. Stress Wave Travel Time vs. Bacterial Infection	49
532. Tensile Strength Perpendicular to Grain and Drying Defects vs. Bacterial Infection and Stress Wave Travel Time	52
6. RESULTS AND DISCUSSION	56
61. Stress Wave Travel Time vs. Bacterial Infection	56
611. Stress Wave Travel Time vs. Bacterial Infection at a Single Analysis Point	56
612. Stress Wave Travel Time vs. Bacterial Infection in a Full-Size Board	58
613. Effect of the Defects in Green Lumber to the Identification of Bacterial Infection by Stress Wave Travel Time	62

614. Capability, Interactions and Rank of the Predictors for Stress Wave Travel Time	63
615. Efficiency of Separating Bacterial and "Normal Boards by Stress Wave Travel Time	65
62. Tensile Strength Perpendicular to Grain and Drying Defects vs. Bacterial Infection and Stress Wave Travel Time	68
621. Tensile Strength vs. Bacterial Infection and Stress Wave Travel Time	68
622. Conditions in the Kiln-Drying Experiment	76
623. Drying Defects vs. Bacterial Infection	80
624. Drying Defects vs. Stress Wave Travel Time	84
625. Capability, Interactions and Rank of the Predictors for Drying Defects	90
7. CONCLUSIONS	91
711. Stress Wave Travel Time vs. Bacterial Infection	91
712. Tensile Strength and Drying Defects vs. Bacterial Infection and Stress Wave Travel Time	93
8. SUMMARY	96
LITERATURE CITED	100
APPENDICES	104
VITA	148

1. INTRODUCTION

The presence of anaerobic bacterial infection in red oak (Quercus sp.) lumber that causes problems for wood processing was verified in the late 1970s (Ward and Zeikus 1980). According to the current knowledge, these bacteria attack standing trees only. The importance of anaerobic bacteria in wood processing comes from the enzymes they secrete that are able to weaken chemical bonds between wood cells. Consequently, infected lumber will often develop surface, end and internal checks, and the incipient ring failure will be aggravated during drying, even under standard mild conditions. The Hardwood Research Council estimated that annual losses due to drying defects related to bacterial infections in oak lumber can affect as much as 500 million board feet annually with resultant monetary losses as high as \$25 million (Ward et al. 1991).

Defect-prone bacterially infected red oak lumber is difficult to detect before drying without the use of costly, time-consuming physico-chemical tests (Ward and Ross 1989), as bacterial infections cannot be easily visually recognized. A rapid, accurate, and inexpensive method for detecting bacteria in green red oak lumber does not now

exist although it is much needed for the wood using industries to reduce drying and related processing costs.

Most of the information available today regarding the chemical alteration of wood by bacteria has been obtained by culture techniques (Ward and Zeikus 1980), microscopy (Sachs et al. 1974), and chemical analysis of extracted materials (Zinkel et al. 1969). Recently, trace vapor detection and ion mobility spectrometry (IMS) were found to be accurate methods to distinguish normal and bacterially infected heartwood of red oak lumber in laboratory conditions (Lawrence 1991). IMS tests are able to produce results in 5 to 10 seconds, but they require preparation of small sliver sample and rapid heating at approximately 200 °C.

This study is a continuation of the research of the U.S. Forest Products Laboratory to develop a nondestructive evaluation technique that can be used at a mill to detect bacterially infected wetwood and predict consequent drying defects in oak lumber (Ward and Ross 1989). If infected wood could be detected and separated from uninfected wood, the infected wood could be dried under milder drying schedules to minimize, or even eliminate, bacterially related drying defects.

2. HYPOTHESES

Prior research on the applications of stress wave analysis (Ross and Pellerin 1991b) has suggested that stress wave travel time across the grain of green red oak lumber could be a realistic method to indicate the bacterial infection and the development of bacterially related drying defects.

It is hypothesized that differences in stress wave travel time (across the grain) reflect differences in tensile strength (perpendicular to the grain). Because bacterial infections weaken the wood, if stress wave travel time is low relatively in a piece of red oak lumber, then the piece is bacterially infected and will likely develop surface, internal and end checks, and aggravate incipient ring failure during drying. It is further hypothesized that if the infection is the more severe (i.e., the higher the percentage of the volume of the piece infected), then the greater the travel time.

3. OBJECTIVES

The objectives of this study are:

1. To establish the relationship between the level of bacterial infection and stress wave travel time in green red oak lumber.
2. To establish the relationship between tensile strength perpendicular to grain and stress wave travel time in bacterially infected and uninfected wood, and to explore the subsequent relationship between the formation of drying defects (surface, internal and end checks, aggravation of ring failure) and stress wave travel time in green lumber.

4. LITERATURE REVIEW

41. Bacterial Infection in Red Oak Wood

411. Occurrence and Causes

Bacterially infected wood is "an abnormal type of heartwood infected with bacteria that can occur within the trunks of living trees" (Ward and Pong 1980). It can occur in both softwoods and hardwoods, but tends to be more prevalent in certain tree species. Bacterial infection has often been related to the presence of wetwood which is defined as "a type of heartwood in standing trees which has been internally infused with water" (Ward and Pong 1980).

A conical pattern of bacterial infection is typical for red oaks in the longitudinal direction: the bacterial infection originates at injuries in the roots or at the root collar, and forms a conical pattern in the central core of the lower bole, tapering to an apex in the upper bole. Wengert (1990) estimated that the bacteria move only a couple of inches a year upward the stem, and it would be rare to find bacterial infection more than 12 feet above the ground in a red oak tree. It appears that the bacteria prefer wetter soils, and

also older trees (more than 75 years old). Red oak trees killed by gypsy moth (Porthetria dispar L.) damage seem to have a much more widespread bacterial infection than healthy trees (Wengert 1990). A study has clearly shown the reduced quality in gypsy moth infected and killed trees (Kersavage 1988).

A striking feature of bacterially infected wetwood is its water-soaked and somewhat darker appearance in comparison with adjacent normal wood (Ward and Zeikus 1980). It does often have an abnormally high moisture content: in red oak, green moisture content can be as high as 110%, compared to the normal 75 to 80% (Wengert 1990). In another study, an average moisture content of 91% was measured for wetwood in green red oak wood, 80 % for normal heartwood and 81% for sapwood (Ward and Pong 1980). A considerable overlapping in MC was reported as well (Ward and Zeikus 1980, Ward and Groom 1983).

The bacteria also create acetic acid and higher fatty acids that have a characteristic unpleasant, rancid odor (Schink and Ward 1984). Propionate, butyrate, valerate, and caproate in fetid liquid were detected from acidic oak wetwood (Ward et al. 1968). The odor is the most noticeable when the wood

is green, but can return if dry wood is subjected to humid conditions. The odor is often accompanied by a strong vinegary smell and vapors that sting one's eyes. In fact, the particular odor is still considered one of the safest detection criteria for bacterially infected wood (Ward and Ross 1989).

412. Related Problems

4121. Shake and Frost Cracks

The anaerobic bacteria in red oaks secrete pectin-degrading enzymes, which are believed to attack and degrade the pectic substances of the compound middle lamella between wood cells, and weaken the intercellular chemical bonds between them (Schink et al. 1981a,b, Ward and Pong 1980, Ward and Zeikus 1980). The secondary cell walls in bacterially infected wood do not appear to be weaker than those in normal wood with similar specific gravity (Ward and Pong 1980). Weaker bonding between the cells of bacterially infected wood means an increased risk for radial and tangential growth ring separations when the affected trees are subjected to stress from wind, growth and freezing (Ward and Pong 1980). These separations, known as shake, are

internal defects of the trunk that often go undetected when the tree appears vigorous and healthy (Ward and Pong 1980).

4122. Reduced Tensile Strength

Tensile strength perpendicular to grain is critical in determining the susceptibility of wood to checking during drying (Youngs 1957). The average tensile strength perpendicular to grain for green southern red oaks was 24 percent lower for bacterially infected heartwood than for normal heartwood (Hart et al. 1984, Ward and Hart 1985). In addition to drying, the reduction in this strength tends to cause problems in machining (Kutscha and Ethington 1962, Wengert 1990).

4123. Drying Degrade

The bacterially weakened wood of practically all species will be likely to develop checks and splits during standard drying conditions (Ward and Ross 1989, Wengert 1990). Checks may be deep surface checks, internal checks called honeycomb, or bottleneck checks which are surface checks that developed into internal checks (Rasmussen 1961).

Because bacterial infection is not the only cause for the aforementioned drying defects, it is difficult to estimate the loss from bacterially infected lumber in the lumber and furniture industries. Ward and Pong (1980) estimated that the annual wood losses from drying defects associated with bacterial infection in oak lumber produced in the Eastern United States are at least three percent. Ward and Groom (1983) estimated that only the kiln drying losses from checks and honeycomb can be three times greater in bacterially infected oak boards than in normal oak boards under similar drying conditions. Eight to twenty-five percent losses in usable lumber volume were observed from honeycomb and ring failure in bacterially infected wood, resulting in monetary losses ranging from \$34 to \$139 per thousand board feet of rough lumber (Ward 1978). Seven to twenty percent of thick, 9/4 red oak lumber estimated to contain more than 60 percent bacterial heartwood was degraded during various drying experiments compared to 0.5 to 2.5 percent in lumber with less than 25 percent bacterial heartwood (Ward and Simpson 1987).

The drying times for green bacterially infected oak lumber tend to be longer than those for uninfected lumber, resulting in increased drying cost. Drying of bacterial

heartwood boards of red oak from 97 % MC and drying of normal heartwood boards from 86 % MC to a final 7% MC required 324 and 312 hours, respectively, when a 4-stage jet drying was used (Ward and Pong 1980). A study on thick, 9/4 red oak lumber indicated that bacterial boards dried at similar rates, but, because bacterial lumber usually had a higher initial green moisture content, its drying took a longer time (Ward and Simpson 1987).

During the early and middle stages of kiln drying, when the drying defects initiate, green bacterially infected oak lumber does not withstand temperature elevations as well as uninfected lumber (Ward and Pong 1980, Wengert 1990). Honeycomb in bacterially infected northern red oak could be minimized by lower initial dry bulb temperatures and depressions (Ward et al. 1972, Ward and Shedd 1979). Bacterial southern bottomland oak lumber, however, developed honeycomb and collapse under the mildest kiln schedules (Ward and Pong 1980).

42. Stress Wave Nondestructive Evaluation of Wood

421. Concepts and Fundamental Theories (Ross and Pellerin 1991b)

Stress wave nondestructive evaluation (NDE) techniques use low stress molecular motions to measure energy storage and dissipation. Energy storage is manifested as the speed at which a wave travels in a material. In contrast, the rate at which a wave attenuates is an indication of energy dissipation.

The propagation speed of stress waves can be determined by coupling measurements of the time between pulses and the length of the travel distance by the following equation:

$$C = 2L / \Delta t \quad (1)$$

where C = Propagation speed
 L = Length of the travel
 distance
 Δt = Time between pulses

Furthermore, the modulus of elasticity can be computed using C and the density of the material:

$$\text{MOE} = C * \rho \quad (2)$$

where MOE = Modulus of elasticity

ρ = Density of the material

A more rigorous treatise on the measurement of energy loss via stress wave techniques is presented by Kolsky (1963). This includes determining the quantity of energy imparted into a member and the corresponding rate of loss of energy. Loss of energy would be calculated using an integral of a waveform, as is done for determining the energy emitted during acoustic emission testing of materials (Harris et al. 1972). This is defined as the root mean square (RMS) value.

For most NDE purposes there are two different wave types that can be propagated in the test material: ultrasonic and impact-induced compressional waves (Kaiserlik 1978). Gerhards (1978) compared both types of induced stress waves with NDE testing of Douglas fir (Pseudotsuga menziesii) wood planks: the pulse transit times of the ultrasonic pulse testing meter and the impact-stress wave timing instrument are comparable.

422. Verifications and Applications

4221. Sound Wood

Wood is neither homogeneous nor isotropic and, hence, the usefulness of one-dimensional wave theory for describing stress wave behavior in wood could be considered dubious (Ross and Pellerin 1991b). Jayne (1959) was the first to hypothesize and verify that the two stress wave properties, energy storage and dissipation, are controlled by the same mechanisms that determine the mechanical behavior of wood. He demonstrated a relationship between energy storage and dissipation properties, as measured by forced transverse vibration techniques, and the static bending properties of small clear wood specimens. Consequently, useful mathematical relationships between these properties and static elastic and strength behavior should be attainable through statistical regression analysis.

Clear wood is composed of many tube-like cells cemented together. At the microscopic level energy storage properties are controlled by orientation of the cells and their structural composition, factors which contribute to static elasticity and strength (Ross and Pellerin 1991b). Such

properties are observable as frequency of oscillation in vibration or speed of sound transmission. Energy dissipation properties, conversely, are controlled by internal friction characteristics to which bonding behavior between constituents contributes significantly.

Pellerin (1965) verified Jayne's hypothesis using free transverse vibration techniques on dimension lumber by analyzing a damped sine wave form and utilizing equations for modulus of elasticity and logarithmic decrement. Measured values of modulus of elasticity and logarithmic decrement were then compared to static MOE and strength values. O'Halloran (1969) obtained comparable results with softwood dimension lumber. Bertholf (1965) was able to accurately predict dynamic strain patterns in small wood specimens, and verify the dependence of propagation velocity on the modulus of elasticity of clear wood.

Kaiserlik (1975), and Kaiserlik and Pellerin (1977) applied stress wave techniques to evaluate the tensile strength of small samples of clear lumber containing varying degrees of slope of grain. Ross (1985) examined wave behavior in both clear wood and wood-based composites and observed nearly excellent agreement with Jayne's hypothesis.

Smulski (1989) was successful to predict static bending MOE and MOR of small, clear, straight-grained beams of four northeastern hardwoods by stress wave velocity. Tanaka et al. (1991) performed corresponding tests on Japanese sugi lumber. Their results showed that both the propagation of ultrasonic waves and impact induced stress waves were able to predict the weakened bending strength and stiffness.

4222. Bacterially Infected Wood

NDE testing using both impact stress wave and ultrasonic pulses was used in a drying study on hemlock-fir dimension lumber with and without bacterially infected wetwood to determine if these techniques could be used as a substitute for weighing to distinguish heavy boards. The NDE measurements were made along the grain of the sample boards in the green condition. Both NDE methods were effective in separating light boards above 100 % MC, but no distinction could be made between bacterial and normal boards with a similar weight.

Reverse results were obtained on the detection of bacterially infected red and white oak wood in the study by Ward et al. (1991). Eighty-four percent of red oak boards

and 45 percent of white oak boards with at least 30 percent infected wood could be correctly detected by the minimum stress wave speed across the grain. Only two and three percent of the uninfected boards were incorrectly detected, respectively. Of the red oak boards with at least 70 percent infected, 93 percent were correctly distinguished. The dissimilar efficiency for red and white oak wood was attributed to differences in the bacterial populations. However, the stress wave travel time or bacterial infection was not related to tensile strength, or actual drying defects.

5. EXPERIMENTAL PROCEDURES

51. Procurement of Material

511. Logs and Lumber at the Saw Mill

Two hundred eighty freshly sawn, 4/4 red oak boards were collected from Ontario Hardwood Co., Inc., Ontario, Virginia on May 21, 1991. The saw mill is located in the Piedmont area of Southcentral Virginia. In this area, wet soils which are known to produce wood with bacterial infection (Wengert 1990) are common, and bacterial infections are frequent.

The lumber was sawn from 32 logs, selected by the owner of the saw mill for likelihood to contain bacterially infected wood. The presence of bacterial infection with logs was determined at the butt end of the log, using rancid odor, occurrence of ring shake, and dark greenish or red-brownish discoloration as criteria (Ward and Pong 1980). To be able to use odor as a sign of bacterial infection, the logs were as freshly-cut as possible. Only butt logs were accepted, because the bacterially infected section is normally limited to the butt part of a red oak bole. The log length was 12 feet. The minimum log diameter was 12 inches to facilitate

an adequate yield of boards with suitable dimensions.

The logs were grade-sawn at the mill. Flat-sawn boards were needed to facilitate an as uniform quality as possible for the strength tests and experimental drying. The 12-foot boards were cross-cut to 6-foot lengths before grading. The 6-foot boards were graded by the saw mill grader for their own purposes, using standard rules of the National Hardwood Lumber Association (NHHLA 1990). When the cross-cut lumber entered the green chain a number to show the original 12-foot board and a letter to show the lengthwise location there was marked on the top section of each board.

Boards with a width of 4 to 6 inches were accepted in order to obtain the planned 240 boards. All No. 1 Common and some No. 2A, 2B and 3A Common boards were accepted to make sure that enough bacterially infected boards were obtained. The lower grade boards tend to come from the core section of log where the bacterial infection is the most probable (Ward and Pong 1980).

The lumber was stacked in two stacks for shipping. To prevent degradation and drying during shipping and storage, the lumber was end-coated with a wax coating (Anchor Seal)

and wrapped with a plastic cover. Insecticide or fungal dip treatment was not used because the amount of stain-prone sapwood was minimal.

512. Lumber Handling at the U.S. Forest Products Laboratory

The lumber was shipped by a commercial carrier to the U.S. Forest Products Laboratory, Madison, Wisconsin. Upon arrival, it was stored at a temperature of 36 °F and relative humidity of 80 % to prevent deterioration. The lumber was kept wrapped in plastic.

Before any experiments, the quality of lumber was visually inspected. Fifty-six boards were rejected because of insufficient clean test area. To compensate this loss of material, 17 boards with a width of 11 inches or more were ripped to two halves. The boards with wane and sapwood were edge-trimmed to their maximum width, to the closest 0.25-inch, that in each case resulted in even edges and minimal amount of sapwood.

In total, 241 individual pieces of lumber were accepted. Ninety-three (39 %) of them were later classified as bacterial, 68 (28 %) as mixed, and 80 (33 %) as "normal"

boards (Chapter 521, p. 21). Furthermore, 160 (66 %) of them were classified as flat-sawn, 65 (27 %) as ripped along the center line, and 16 (7 %) as quarter-sawn (Fig. 2, p. 23). The mean board width was 6.1 inches, and 204 (85 %) of the boards were 5 inches or wider.

52. Data Collection Details

521. Establishing the Presence of Bacterial Infection

Defining the presence and especially the severity of bacterial infection encounters both hypothetical and technical problems. The presence of bacterial population can be detected definitely, but defining the actually harmful population is more complicated. This issue is closely related to the severity of infection. The severity can be evaluated with different methods. First, degree of pectin degradation can be measured, but this is a technically difficult procedure. Second, moisture content in the bacterially infected area can be used, but as reported, for red oak wood there is a considerable overlapping between the moisture content of bacterially infected and uninfected wood. Third, estimating the extent of infection in a board by odor and color can be used, even though this procedure is

subject to error (i.e. pieces may be missed) when the wood is only partially or mildly infected.

Sensing bacterial infection by odor and discoloration was used to determine the presence of bacterial infection in this study. Rancid, fruity, or heavy vinegar smell, and green or reddish-brown discoloration were considered signs of bacterially infected wood.

Each of the 241 accepted boards were examined and the zones and signs of certain, possibly mild and no infection were marked on both faces. The infection classes had the following characteristics:

	Odor	Discoloration
Certain Infection	Strong	Obvious
Possibly Mild infection	Not strong, not normal	Not strong, not quite normal
<u>No Infection</u>	<u>Normal</u>	<u>Normal</u>

The extent of the infection was estimated as the percentage infected volume, which was used to classify boards as:

Bacterial: More than 70 percent certainly or possibly mildly infected.
Mixed: 30 to 70 percent certainly or possibly mildly infected.
"Normal": Less than 30 percent certainly or possibly mildly infected

The capability of the average board moisture content to predict the severity of infection and improve the ability of stress wave analysis to indicate bacterial infection was tested, as well.

A map of both faces of each board was drawn, showing the zones and signs of bacterial infection. Though considered a difficult and somewhat unreliable procedure, this was used to establish the presence of infection at each point located at 1-foot interval along the length of the board, where the stress wave analyses were to be performed (Chapter 524, p. 35-39). Each point was then classified as certainly infected, possibly mildly infected, or uninfected. The points were numbered and marked with a single line on the face and the edges so that subsequent tests could be done at the same location. The grain pattern, natural defects (knots, checks, splits, wormholes, decay, wane) and the zones of sapwood, which were to be considered in the subsequent tests, were marked on the map as well. Examples of a map and the different grain patterns are exhibited in Figs. 1 and 2, respectively (p. 23).

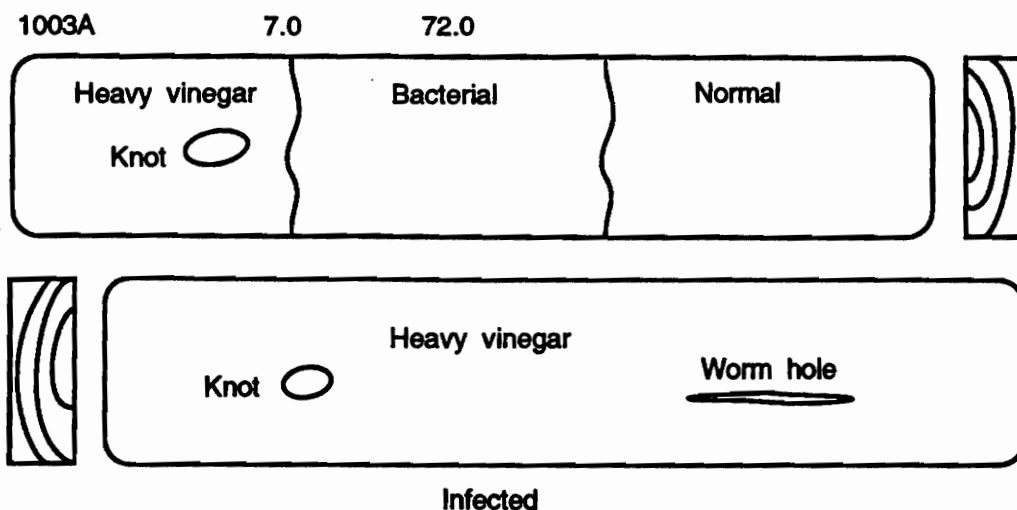


Fig. 1. Example of a Board Map.

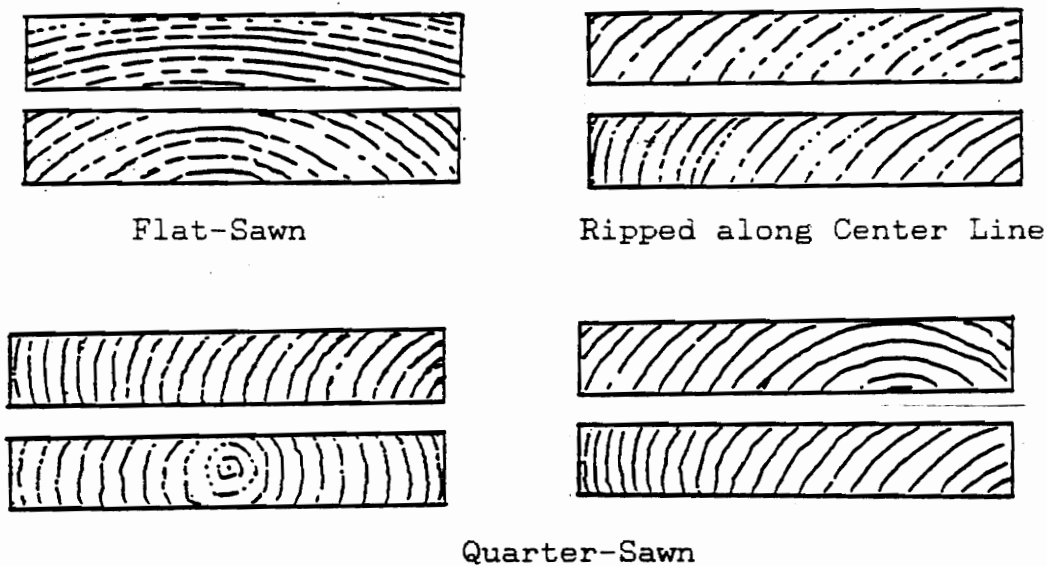


Fig. 2. Examples of Different Grain Patterns in the Material of Red Oak Lumber (Adopted from: Ward and Ross 1989)

522. Verifying the Presence of Bacterial Infection

The presence of bacterial infection was verified by scanning electron microscopic (SEM) examinations on small specimens cut from samples of certain infection, possibly mild infection and no infection. A 2-inch specimen was cut from the butt end of each board in a green condition, marked with an identification number, wrapped in an aluminum foil, and kept in a freezer (temperature of 0 °F) until the actual examination. There were two reasons to cut the samples from the butt end only: first, bacterial infection is the most probable here, and second, cutting more samples would have reduced too much the length of the board.

Specimens from 50 boards were then chosen for the actual SEM examinations using a stratified random sampling, where the strata were the three bacterial infection classes for the board by sensing. Ten boards were randomly sampled for the strata "Bacterial boards" and "Normal boards", and 30 boards for the stratum "Mixed boards".

The guidelines by McGinnes et al. (1974) and Sachs et al. (1974) were followed in the SEM verification. For preparing the slices for SEM viewing, samples of 0.5-inch in radial

and tangential and one inch in longitudinal direction were cut. The isolated specimens were immediately submerged in a four percent buffered gluteraldehyde phosphate aqueous solution to fix the structure of the bacteria, i.e. to prohibit biological changes. After being kept sealed in the solution in a refrigerator temperature two days, the isolates were removed and dehydrated in a series of increasing concentrations of ethanol (70 to 100 percent). The final ethanol solvent was removed by critical point drying with carbon dioxide. The dried specimens were cut radially to 0.2 to 0.4 inch diameter slices which were then gold-coated to facilitate electron conductivity and prevent unnecessary warming of wood during SEM viewing which could cause cracks in wood.

The SEM studies were performed by using a magnification of 2,500 to 10,000. The most typical cases were photographed. The presence of bacteria in a sample was recorded. Bacteria were particularly looked for on the pit margins of the lumen walls of vessels, where the bacteria tend to attack readily (Ward 1991 Personal Communication). The severity of the infection was evaluated visually by using the severity classes heavy, present and no infection. Heavy infection was indicated by large localized bacterial populations (Fig. 3a,

p. 28), or moderate populations throughout the sample (Fig. 3b, p. 28), as well as by distinct cracks and slime on cell wall (Fig. 3c,d; p. 29). Present infection was indicated by less abundant bacteria (Fig. 4a, p. 30) but also by abundant tyloses in vessels (Fig. 4b, p. 30). Uninfected samples were to have no bacteria.

Results on the comparison of sensing and SEM detection of bacterial infection are shown in Table 1 (p. 31). The butts of all boards with an estimated infected volume of more than 70 percent (bacterial boards) had a heavy infection. None of the butts of the boards evaluated to be free from bacteria had an infection, and the other "normal" boards, with an estimated infected volume of 10 to 30 percent, had only a present infection. The only actual errors in sensing were observed for the butts of mixed boards with an estimated infected volume of more than 30 but less than 70 percent: no infection was observed in 17 percent of them. Of the truly infected samples of mixed boards, 92 percent had only a present infection. This indicated that the boards sensed as mixed resembled "normal" rather than bacterial boards.

Further verification on the presence of bacterial infection was performed by a paired comparison of SEM results on

subsequent boards from a log (Table 2, p. 31). For each pair, the severity of infection decreased or remained unchanged from butt to top both by sensing and SEM detection. Furthermore, 90 percent of the boards sensed as bacterial and 83 percent of the boards identified by SEM as heavily infected were butt boards. These results were consistent with the reported conical form of bacterial infection within a trunk that starts from the root collar.

The comparisons only verified the presence of bacteria in a butt of a board, thus not facilitating a generalization for a full-size board. The SEM samples comprised only 11 percent of boards sensed as bacterial and 13 percent of boards sensed as normal, but as much as 44 percent of boards sensed as mixed, whose identification was expected to be the most uncertain. In sensing, the percentage infected volume of a board was estimated with an accuracy of ± 10 percent only, and the actual accuracy was most likely worse. On the other hand, a mild bacterial infection should not necessarily result in harmful changes in wood properties for processing (Ward 1991 Personal Communication). Thus, possibly the identification of heavy infection only has an actual importance.

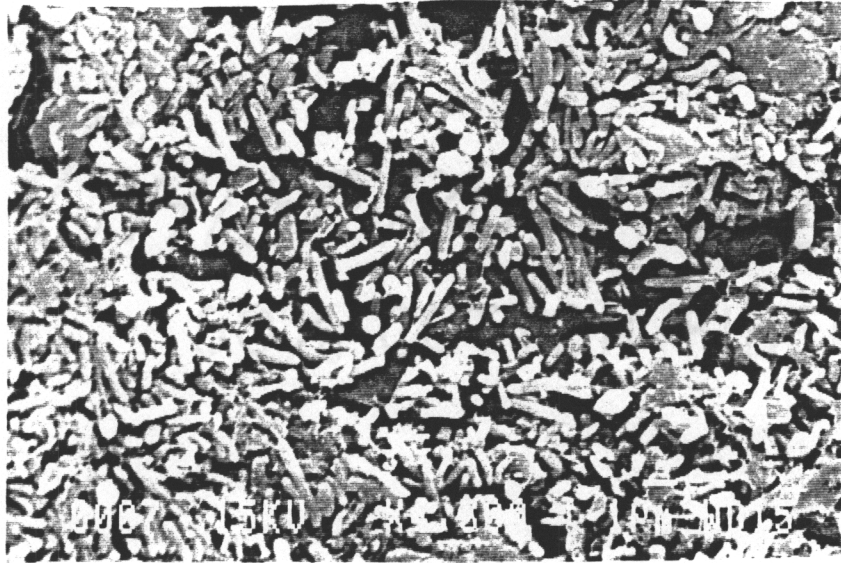


Fig. 3a. Heavy Bacterial Infection in the Red Oak Heartwood with a Large Localized Bacterial Population.

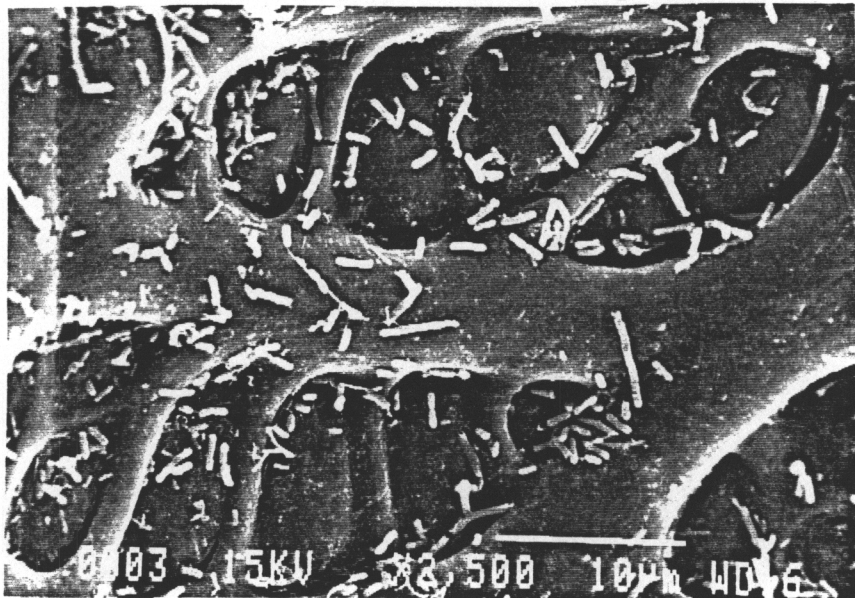


Fig. 3b. Heavy Bacterial Infection in the Red Oak Heartwood with a Population Throughout the Sample.

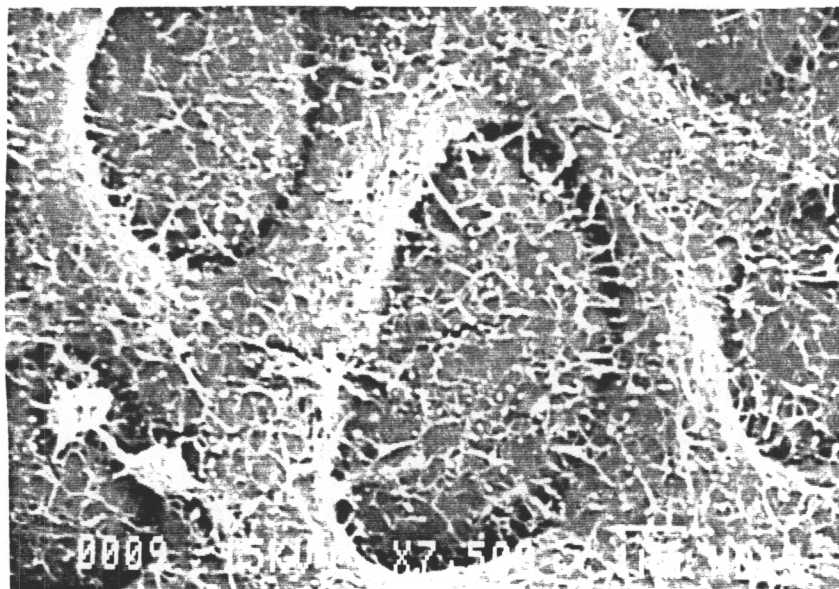


Fig. 3c. Cracks and Slime on the Vessel Wall in the Red Oak Heartwood with a Heavy Bacterial Infection.

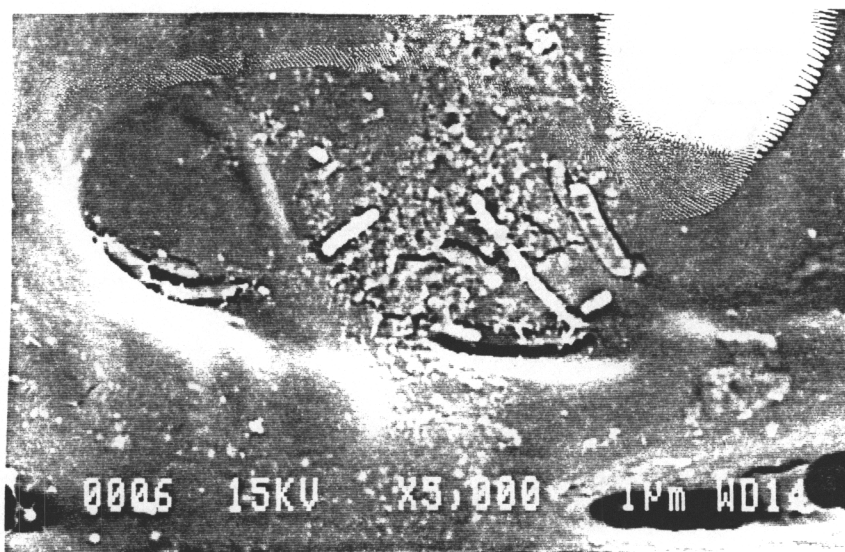


Fig. 3d. Severe Cracks on the Vessel Wall in the Red Oak Heartwood with a Heavy Bacterial Infection.

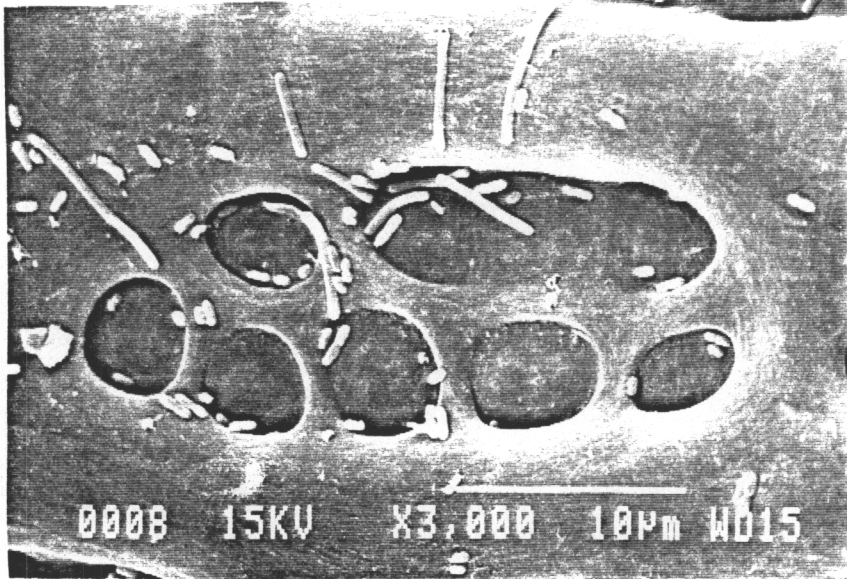


Fig. 4a. Relatively Mild Bacterial Infection in the Red Oak Heartwood.

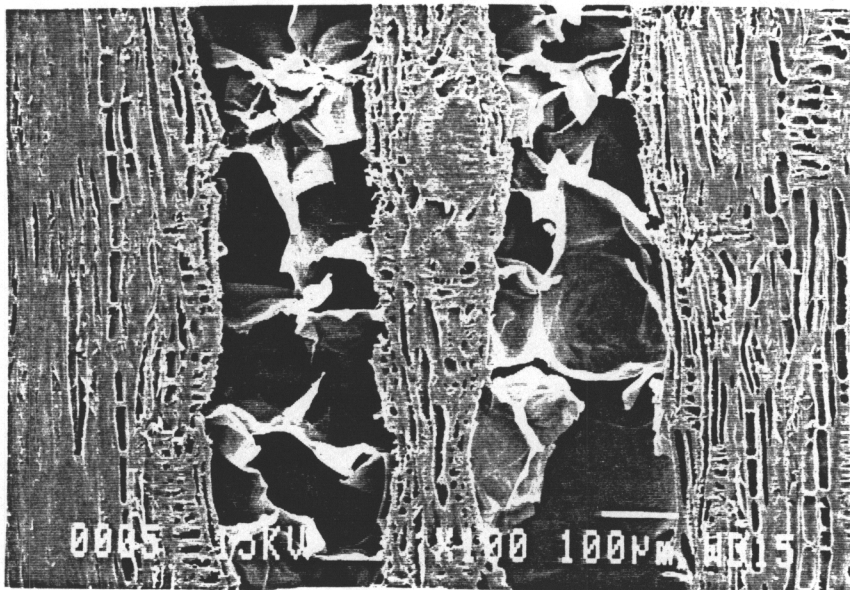


Fig. 4b. An Abnormal Abundance of Tyloses in the Vessels of the Red Oak Heartwood.

Table 1. Comparison of the Results on Sensing and Scanning Electron Microscopic (SEM) Identification of Bacterial Infection in a Butt of a Board.

Infection in a Board	Result of Sensing		Result of SEM		
	Infected Volume	#	Severity of Infection		
			Heavy #	Present #	No #
Bacterial	100	8	8	0	0
	90	1	1	0	0
	80	1	1	0	0
Mixed	60	3	0	3	0
	50	20	2	15	3
	40	4	0	3	1
"Normal"	30	3	0	2	1
	20	1	0	1	0
	10	1	0	1	0
	0	8	0	0	8

Table 2. Paired Comparison of the Results on the Sensed and SEM Identified Bacterial Infection in Two Subsequent Boards from a Log.

Pair	Butt Board			Top Board		
	Sensed		SEM	Sensed		SEM
1	Bact.	100 %	Heavy	Bact.	100 %	Heavy
2	Bact.	100 %	Heavy	Mixed	60 %	Present
3	Bact.	100 %	Heavy	Mixed	50 %	Heavy
4	Bact.	100 %	Heavy	Mixed	40 %	Present
5	Bact.	100 %	Heavy	Mixed	30 %	Present
6	Bact.	100 %	Heavy	Mixed	30 %	No
7	Bact.	100 %	Heavy	Mixed	40 %	Present
8	Bact.	90 %	Heavy	Mixed	60 %	Present
9	Bact.	80 %	Heavy	"Normal"	20 %	Present
10	Mixed	60 %	Present	"Normal"	0 %	No
11	Mixed	50 %	Heavy	"Normal"	0 %	No
12	Mixed	50 %	Present	"Normal"	0 %	No
13	Mixed	30 %	Present	"Normal"	0 %	No
14	"Normal"	0 %	No	"Normal"	0 %	No
15	"Normal"	0 %	No	"Normal"	0 %	No

523. Measurement of Moisture Content and Density

To estimate both the average and localized moisture content in a board, a 1-inch along the grain, full width and thickness sample was cut from butt and top end of each board. Moisture content was then determined for each sample with a standard technique (Wengert 1990). The average moisture content was computed for each board as an average of the butt and top end samples.

The specimens used to determine the average moisture content were used to determine the average green and basic density of board, as well. For this purpose their volumes were measured by immersing the specimens in pure, 39 F water and recording the increase in the weight of the container with water, g. The volumes of the tensile strength test specimens were determined by a product of width, thickness and length measured with a caliper (accuracy 0.001 cm).

The mean moisture content, green density and basic density in the board material were 85.1% MC, 65.9 lbs/cu.ft and 35.8 lbs/cu.ft. These were close to the reported values for Northern and Southern red oak. Their heartwoods have normally green moisture contents of 80% MC and 83% MC,

respectively (Wood Handbook 1987). Their normal specific gravities on green volume basis are 0.56 and 0.53 (Wood Handbook 1987). These correspond to the basic densities of 34.9 and 33.1 lbs/cu.ft., and to the green densities of 62.9 and 59.6 lbs./cu.ft. assuming the aforementioned normal values of moisture content.

No significant difference was observed in moisture content ($p = 0.57$), green density ($p = 0.17$) or basic density ($p = 0.31$) between bacterial, mixed and "normal" boards (Table 3, p. 34). Thus, these variables could not be used to evaluate the severity of bacterial infection in a board. This result was consistent with the results from prior research on red oak (Ward and Pong 1980).

The aforementioned results on moisture content were presumed to underestimate the actual average moisture content in a board, because the ends of the board were apt to rapidly lose moisture when exposed to drying conditions. This along with the subsequent difference in green density might hinder the interpretation of the results from stress wave analysis (Chapter 524, p. 35-39).

Table 3. Moisture Content, Green Density and Basic Density of a Board by Bacterial Infection Class, as Determined by the Top and Butt End Samples.

Bacterial Infection Class of a Board	Moisture Content %	Green Density lbs./cu.ft.	Basic Density lbs./cu.ft.
Bacterial	85.8	66.2	35.8
Mixed	84.5	66.4	36.2
"Normal"	84.8	65.3	35.5

Table 4. Estimates for the Moisture Content, Green Density and Basic Density of a Board by the Two Sampling Methods.

Sampling Method	Moisture Content %	Green Density lbs./cu.ft.	Basic Density lbs./cu.ft.
Top and Butt End Samples	85.8	65.8	35.8
Six Samples along the Length of the Board	91.5	66.2	34.1

To check if the underestimation did occur, a test was performed on the 40 boards cut for tensile strength tests (Chapter 525, p. 40-41) to compare the average moisture content and green density by top and butt end samples with that by the six small specimens cut along the length of the board. The difference in basic density was tested as well. A significant ($p = 0.05$) drying did occur (Table 4, p. 34). However, it did not affect the interpretation of stress wave results, because the rank or difference between single boards was not changed. No significant difference was found in green or basic density ($p = 0.5$).

The possibility that moisture content, green density or basic density would have effect to the results of stress wave analysis was examined. No relationships were observed: R-Squares were only 0.049, 0.034 and 0.025, respectively. The result on the effect of moisture content was consistent with the observation by Ross and Pellerin (1991a) on green Douglas-fir dimension lumber beyond 75% MC.

524. Stress Wave Analysis

Stress wave analysis was performed on every board. The stress waves were always induced on the face closest to the

bark. The points for the stress wave analysis were located at 1-foot interval along the length of board. The first point was located at 6-inch distance from the original butt (i.e. at 3-inch distance after cutting the samples for the verification of the presence of bacteria and measurement of moisture content and density). However, if any observable defect (knot, cross grain, check, split, incipient ring failure, pith, decay) was noted at the predetermined point, an additional stress wave analysis was performed at the closest point where the wood was judged to be free from the influence of the defect. The defects were recorded in accordance with the classification system by Ward and Ross (1989) (Appendix 1). All stress wave analysis points were numbered on the face and edges of the board for the subsequent tests.

Stress wave analysis was performed at each point by using both the fixed 4-inch stress wave travel distance and the maximum distance allowed by the width of the board. This was 0.5 inch less than the actual width. Boards 5 inches or narrower were analyzed with the fixed distance only. The fixed distance had the characteristic that the flattest-sawn section across the board width could be chosen for the stress waves to travel, and thus effect of varying grain

pattern could be reduced when comparing various readings. The method relied on measured distance, and thus the relative error could be larger when the distance was short. The second method had the marked characteristic that almost the whole board cross-section could be considered.

Stress waves were induced into the wood by an impact hammer, and the transit time was measured in microseconds (μ sec) with a Metreguard No. 239A SN 86003 stress wave timer (Figs. 5a,b,c, p. 38-39). As a result of the lumber dimensions and the test set-up, the effective zone of each stress wave measurement was 1.1 inches in thickness, 4 to 9.5 inches in width, and 3 to 4 inches along the grain. The accuracy of stress wave timing was ± 2 usec, or $\pm 0.1\%$ to 1% (Ross 1991 Personal Communication).

One thousand four hundred forty-five basic stress wave analyses and 201 additional analyses because of the occurrence of defects were performed using the 4-inch travel distance. When using the maximum possible travel distance, 1067 basic and 163 additional analyses were performed.

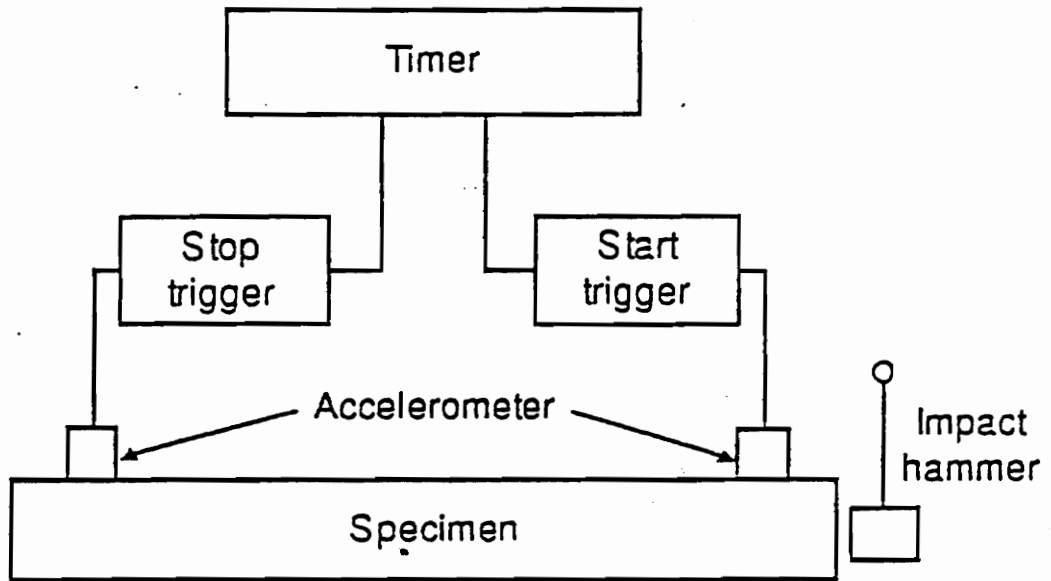
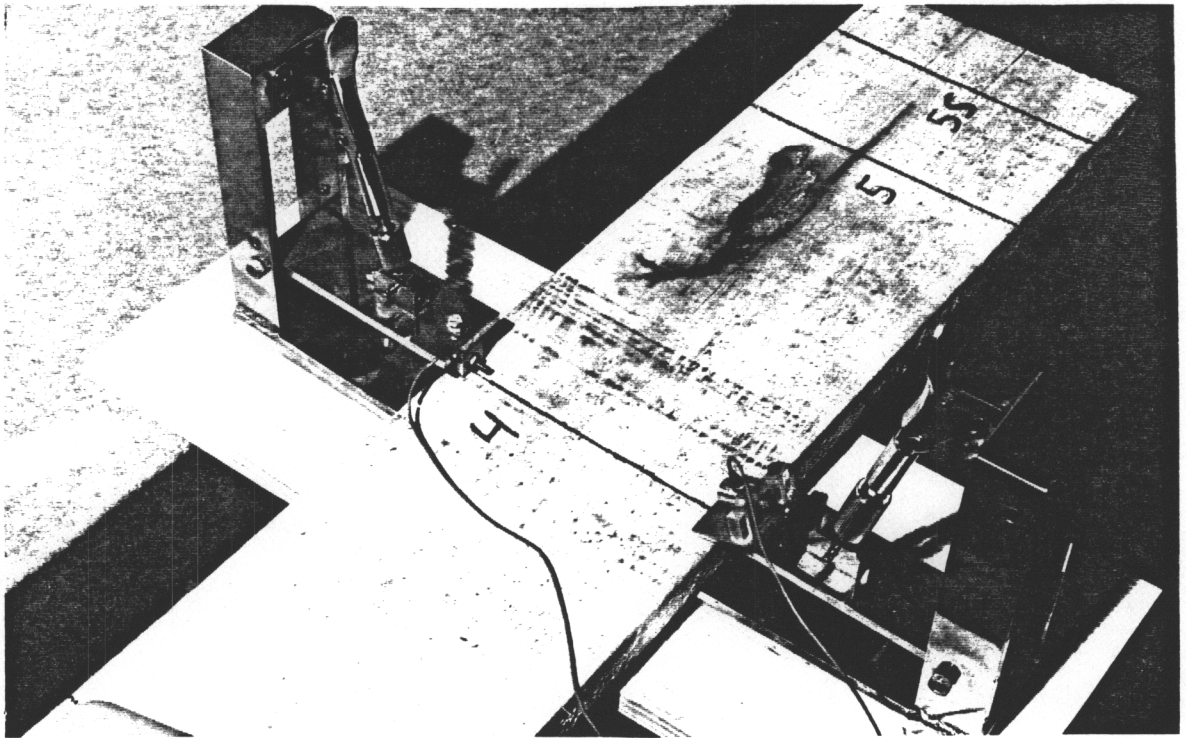
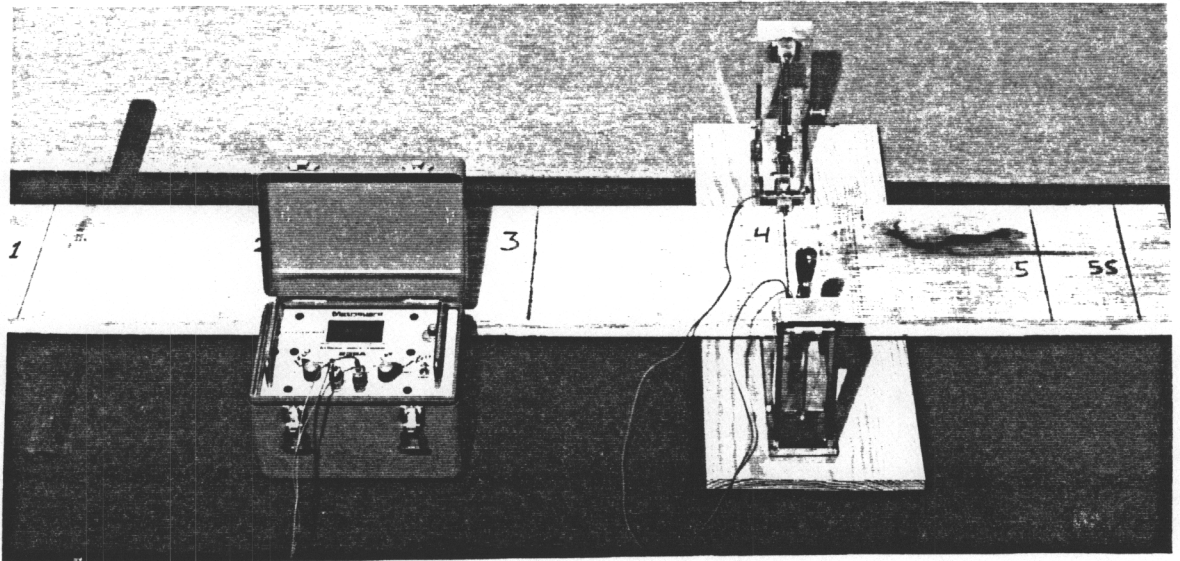


Fig. 5a. Technique to Measure Impact-Induced Stress Wave Travel Time in Wood and Wood Products (Ross and Pellerin 1991b).



Figs. 5b, c. The Stress Wave Timing Procedure and Equipment.

525. Tensile Strength Tests Perpendicular To Grain

Tensile strength perpendicular to grain was measured on small specimens cut from flat-sawn lumber. The tests were performed in a green condition. Based on the U.S. Forest Products Laboratory's experiences from tests on Southern pine (Kretschman 1991 Personal Communication), the specimens of 1 inch in radial, 0.5 inch in longitudinal and at least 5 inches in tangential wood direction were used.

Specimens were cut from a subsample of 40 boards. All boards in the material were ranked by the maximum stress wave travel time in clear wood, on the maximum possible travel distance. Beginning from the board with the longest stress wave travel time, the first board, and after that every second board were chosen until 20 flat-sawn boards with a width of six inches or more were obtained. A corresponding ranking was done by the minimum stress wave travel time, and 20 boards were chosen, beginning from the board with the shortest stress wave travel time. This was to make sure that a sufficient number of specimens with a high and low stress wave travel time were obtained, and that the whole range was covered in the materials for both the tensile strength tests and the kiln-drying experiment.

The boards were surfaced and the test specimens were cut with a band saw from the sections which were examined with stress wave analysis and which were free from visible discontinuities, knots and decay. The edges of the specimens were sanded to remove splinters which might cause an erroneous underestimate of tensile strength. In total, 244 test specimens were cut. They comprised 139 (57 %) certainly infected, 37 (15 %) possibly mildly infected, and 68 (28 %) uninfected specimens.

The tension tests were performed with the hydraulic Universal Screw Power Testing Machine of the U.S. Forest Products Laboratory (Fig. 6a, p. 42). The distance at which the clamps held the specimen was 0.75 to 1.5 inches at both ends (Fig. 6b, p. 43). The actual loading velocity was 0.025 inches/min. The load at which the tension failure occurred was recorded with a Riehle Recorder Model RD-5B, which was calibrated in June 1989. A load cell BLH Electronics Type U3-G1 with a capacity of 500 lbs. was used to record the load. The development of the applied load was plotted separately for each specimen. The cross-sectional area for the computation of maximum tensile stress was determined as a product of width and thickness measured with a caliper at three points (accuracy 0.001 cm).

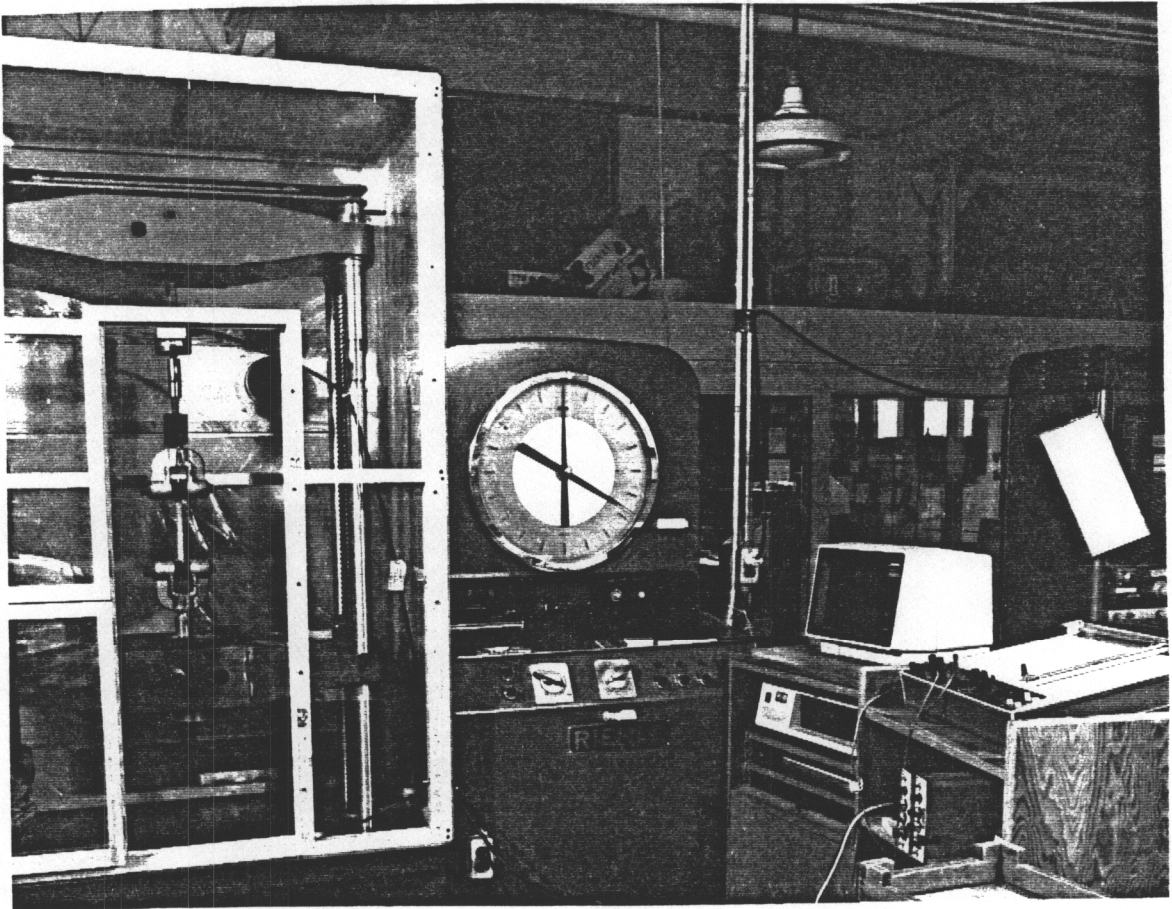


Fig. 6a. The Machinery for Tensile Strength Tests: Universal Screw Power Testing Machine Equipped with a 500 lbs. Load Cell (Left), Riehle Recorder (Between), and Plotter (Right).

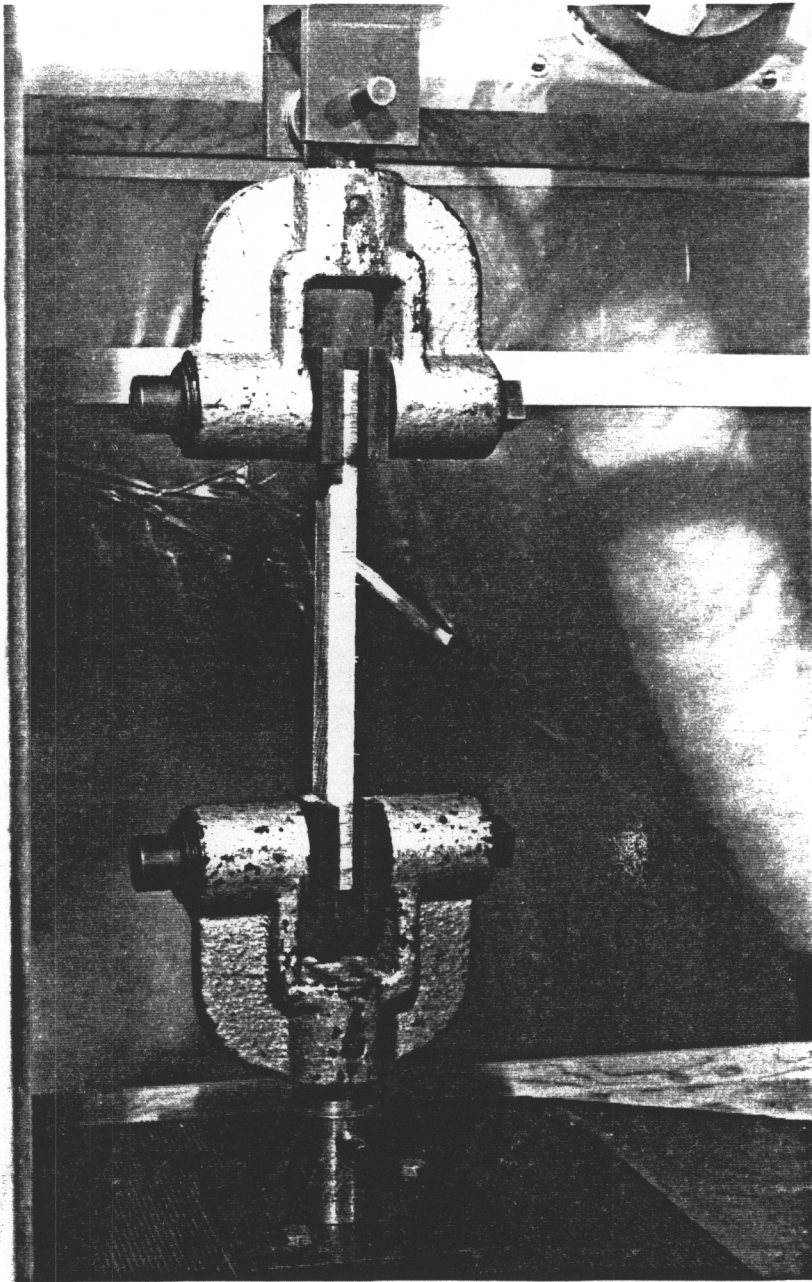


Fig. 6b. A Specimen Ready for a Tensile
Strength Test.

For each specimen, the location and roughness of the failure plane was visually observed, and the specimens were classified to compare the failure pattern between the three bacterial infection classes. The classes were:

- 1 = Strictly along a wood ray (tension)
- 2 = Rough failure across the specimen, through several parallel wood rays (incomplete tension)
- 3 = Strictly along early wood - late wood interface (shear)
- 4 = Combination of 1 and 3 (tension and shear)

526. Kiln-Drying Experiment

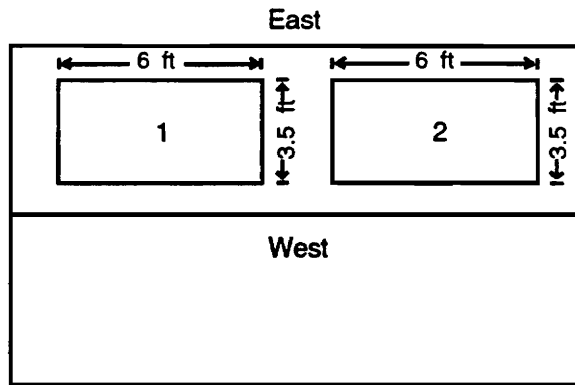
The 201 boards remaining after picking the boards for tension tests were used for a kiln-drying experiment. They comprised 72 (36 %) bacterial, 63 mixed (31 %), and 66 (33 %) "normal" boards. One hundred twenty-two (61 %) of the boards were flat-sawn, 63 (31 %) ripped along the center line, and 16 (8 %) quarter-sawn.

The experiment was performed by using a steam-heated, masonry kiln with a capacity of 4 Mbf. Two stacks of lumber were placed in the kiln. Ten sample boards were cut to monitor the moisture content and degradation of lumber during drying (Table 5, p. 45; Fig. 7, p. 46). The sample

Table 5. Characteristics of Sample Boards.

#	Width inches	Grain Pattern	Bacterial Infection		Green MC %
			Class	Percentage Infected	
1	8.0	Flat-Sawn	"Normal"	20	77.5
2	4.5	Flat-Sawn	"Normal"	0	95.0
3	6.0	Ripped along Center Line	"Normal"	10	84.9
4	4.5	Quarter-Sawn	"Normal"	0	94.1
5	7.0	Flat-Sawn	Bacterial	100	87.2
6	4.5	Flat-Sawn	Bacterial	100	94.1
7	6.0	Flat-Sawn	Bacterial	100	83.7
8	5.0	Flat-Sawn	"Normal"	0	70.8
9	6.0	Ripped along Center Line	"Normal"	0	87.3
10	5.5	Flat-Sawn	"Normal"	0	77.3

Lumber stacks in the kiln seen from above position



Location of sample boards

Stack 1

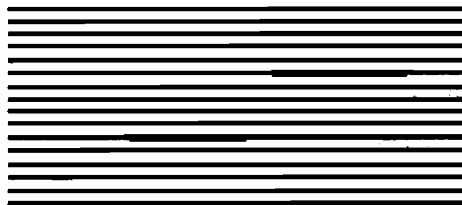


West



East

Stack 2



West



East

Fig. 7. Location of Sample Boards in Lumber Stacks in the Kiln-Drying Experiment.

boards were chosen to simulate a normal kiln charge where the proportion of bacterially infected lumber is relatively small. Otherwise the sample boards were to represent lumber with both easy and difficult, and fast and slow drying (narrow and wide, flat-sawn and quarter-sawn). The sample boards were carefully end-coated to facilitate drying conditions comparable to those of full-size lumber. The monitoring and computations needed were performed with a methodology described by Wengert (1990).

Drying was performed following the standard industrial schedule T4D2 (Rasmussen 1961). It took 28 days (638.5 hours). In the beginning of the experiment, the air velocity was measured at 10 points across the width of the stacks. The measurements showed an average of 355 fpm, with a range of 310 to 410 fpm.

527. Evaluation of Drying Defects

After drying the presence of both the external (visible) and internal (hidden) defects and their severity was recorded. First, end checks and splits were examined on full-size lumber, and those observed were compared to the initial defects mapped while evaluating the lumber (Chapter 521, p.

22). Only the obviously drying-induced checks and splits were recorded. To examine the internal defects, boards were cross-cut along the lines where stress wave analyses were performed. Observable internal checks (called honeycomb), surface checks, end checks and splits, and ring failure, and their severity were recorded at each analysis point, in accordance with the classification system by Ward and Ross (1989) (Appendix 1).

The percentage of the degraded volume of board was estimated to the closest 10 percent, considering all observable external defects and the observable internal defects at clear points only. A 3-inch wide and 2-foot long piece was considered the smallest usable cutting in a board.

53. Data Analysis

531. Stress Wave Travel Time vs. Bacterial Infection

The analysis of the data of stress wave travel time was divided into two parts: at a single analysis point, and in a full-size board. Quarter-sawn material was rejected from the analysis, because it was expected to affect the stress wave travel time (Ross 1991 Personal Communication). Because no

difference was observed in the relative stress wave travel time between the bacterial infection classes when performing the stress wave analysis at the 4-inch nominal or at the maximum possible travel distance, the final results were based on the latter, more comprehensive analysis method.

Common statistical parameters for distribution, location and variation of the stress wave travel time at a single analysis point were computed by bacterial infection class. Because the distributions showed distinct deviations from a normal distribution especially among certainly infected points (Appendix 2), nonparametric Kruskal-Wallis tests (Steel and Torrie 1980) were performed to examine the statistical differences between the bacterial infection classes.

Sign, sign rank and paired t-tests (Steel and Torrie 1980) were performed to examine the difference in the stress wave travel time between a point with a defect and an adjacent point without a defect (Appendix 3). The tests were to show whether the occurrence of discontinuities in the wood structure, which cause gaps to speed of sound transmission, would increase and whether the occurrence of knots, whose higher density compared to adjacent normal wood results in

more inductive material for stress waves, would decrease the stress wave travel time. These issues may have importance for evaluating the results from different studies.

Stress wave travel times at different analysis points along the length of the board were compared between the butt boards (0 to 6 ft from the log butt) and the top boards (6 to 12 ft from the log butt) and by bacterial infection class to show if stress wave travel time decreased toward the top end. This decrease was anticipated because the bacterial infection normally starts from the root collar. The decrease in stress wave travel time should also be larger for bacterial than "normal" boards.

Common statistical parameters for distribution, location and variation of the mean and maximum stress wave travel time were computed for a full-size board by bacterial infection class. Kruskal-Wallis tests were used again, because the distributions especially among the bacterial boards distinctly deviated from a normal distribution (Appendix 4). A simple regression analysis was performed to show the relationship between the mean and maximum stress wave travel time in a board by the estimated percentage of bacterially infected wood of the board volume.

Correlation analysis was performed on stress wave travel time and its potential predictors to show their capability and interactions. Stepwise regression analysis was performed to rank the predictors and show their overall ability to predict stress wave travel time in this material.

Finally, it was computed how large a percentage of the boards detected as bacterial and "normal" could be identified correctly by using fixed limiting values of mean and maximum stress wave travel time in a board.

532. Tensile Strength Perpendicular to Grain and Drying Defects vs. Bacterial Infection and Stress Wave Travel Time

For the tensile strength test material, common statistical parameters were computed for the distribution, location and variation of stress wave travel time on the maximum possible travel distance, maximum tensile stress and failure pattern, by bacterial infection class. The distribution plots (Appendix 5) showed deviations from a normal distribution in some cases, and thus Kruskal-Wallis tests were used. The differences in failure pattern distribution were verified with Chi-Square tests.

Common statistical parameters were computed for and Kruskal-Wallis tests performed on stress wave travel time and maximum tensile stress by failure pattern grouping, as well. Simple linear regression analyses were performed to predict maximum tensile stress by the stress wave travel time, for the whole data and separately for the bacterial infection classes. Correlation analysis was performed to show the capability and interactions of the variables examined. Stepwise regression analysis was performed to rank the potential predictors and show their overall ability to predict stress wave travel time in this material.

The analysis of drying defects by bacterial infection was divided into two parts: defect formation at the points where the stress wave analysis was performed, and in a full-size board as a whole. Quarter-sawn material was rejected from the analysis, and the final results were based on stress wave analysis at clear points only, using the maximum possible travel distance.

Because the sampling of boards for tensile strength tests was suspected to result in a subsample for the drying experiment that was not straightly comparable to the sample for stress wave analysis, the validity of the conclusions of

the relationship of stress wave travel time to bacterial infection based on the whole material was checked within the subsample for drying.

The distributions of stress wave analysis points to the different classes of severity were computed for each particular defect by bacterial infection class, and Chi-square tests were performed to show the statistical differences. All computations and tests were performed on the presence of any bacterially related drying defect as well. The points were classified to three categories by stress wave travel time using the class limits which separated strong, intermediate, and weak specimens in tests on tensile strength perpendicular to grain. Then, the distributions of the stress wave analysis points to these categories were computed for each defect variable, and Chi-square tests were performed to show the statistical differences.

For full-size boards, new defect variables were created which showed the formation of the particular drying defect at any point in the board, and its maximum severity. Computations and tests corresponding to those at single analysis points were performed to show the differences

between bacterial, mixed, and "normal" boards. Common statistical parameters for distribution, location and variation of the percentage of degraded wood of board volume were computed separately for bacterial infection class. Deviations from a normal distribution could be seen in every category (Appendix 6), thus making it necessary to use Kruskal-Wallis tests. The effect of the extent of bacterial infection in a board was examined by a simple linear regression analysis between the percentage of degraded wood, and the percentage of bacterially infected wood.

The boards were classified into three categories by using the limiting values of stress wave travel time that separated strong, intermediate, and weak specimens in tensile strength tests. Then, the distributions of boards into these categories were computed and Kruskal-Wallis tests were performed. Simple linear regression analyses were performed to show the relationships between the percentage of degraded wood in a board, and the mean and maximum stress wave travel time.

Correlation analysis was performed on the degrade percent and the potential predictors to show their capability and interactions. Stepwise regression analysis was performed to

rank the predictors and show their ability to predict the degrade percent in this material.

6. RESULTS AND DISCUSSION

61. Stress Wave Travel Time vs. Bacterial Infection

611. Stress Wave Travel Time vs. Bacterial Infection at a Single Analysis Point

Detailed results on stress wave travel time at a single analysis point by bacterial infection class are shown in Appendix 7. Clear points in flat-sawn lumber sensed as certainly infected had an eight percent longer stress wave travel time than those sensed as possibly mildly infected or uninfected (Table 6, p. 57). This difference was statistically significant ($p = 0.0001$), even though the absolute difference was only 25 $\mu\text{sec}/\text{ft}$. The approximately equal stress wave travel time at possibly mildly infected and uninfected points indicated no actual difference between them in the extent of the infection.

The somewhat uncertain accuracy of sensing the bacterial infection (Chapter 522, p. 24-31) must be realized when interpreting the results; those for the possibly mildly infected points in the first hand. Moreover, when the number of observations is as high as in this sample, even small

Table 6. Stress Wave Travel Time at a Clear Analysis Point by Bacterial Infection Class, at the Maximum Possible Stress Wave Travel Distance.

Bacterial Infection	Stress Wave Travel Time $\mu\text{sec}/\text{ft}$
Certain	319
Possibly Mild	294
No	295

Table 7. Stress Wave Travel Time in a Clear Wood of a Full-Size Board by Bacterial Infection Class at the Maximum Possible Stress Wave Travel Distance.

Bacterial Infection Class of a Board	Stress Wave Travel Time $\mu\text{sec}/\text{ft}$	
	Mean	Maximum
Bacterial	323	377
Mixed	297	316
"Normal"	298	316

numerical differences may appear statistically significant.

612. Stress Wave Travel Time in a Full-Size Board vs. Bacterial Infection

Detailed results on mean and maximum stress wave travel time in a board by bacterial infection class are shown in Appendix 8. The results followed the same guidelines as those for single analysis points: bacterial boards had longer stress wave travel times than mixed and "normal" boards, and the difference was significant ($p = 0.0001$) (Table 7, p. 57). The difference was the largest, 60 $\mu\text{sec}/\text{ft}$, for the maximum stress wave travel time. Ward and Ross (1989) observed stress wave travel times as high as 700 to 1500 $\mu\text{sec}/\text{ft}$ for heavily infected Northern red oak lumber, and 300 to 340 $\mu\text{sec}/\text{ft}$ for uninfected lumber. The considerably longer stress wave travel time for infected lumber in this preliminary study compared to my study was attributable to the different set-up for stress wave analysis: Ward and Ross (1989) did not omit the observations at points with a defect, such as shake which is typical for bacterially infected red oaks and results in excessively long stress wave travel times.

A decrease in stress wave travel time was observed from the butt to the top of a board, and the decrease was sharper in bacterial than other boards (Fig. 8, p. 60). Moreover, the decrease was sharper in the butt than the top boards (Fig. 9, p. 61). The results indicated a decrease in the severity of infection along the length of a board. This was consistent with the current knowledge of the naturally conical form of bacterial infection within a trunk initiating from the root collar.

No relationships were found between the mean and maximum stress wave travel time and the estimated percentage of bacterially infected wood of the board volume: R-Squares were 0.016 and 0.089. This result, which was opposite to that from the comparison of bacterial infection classes, suggested that the real accuracy when estimating the infected volume in a board was worse than the $\pm 10\%$ used in the estimation. However, the regressions had p values of 0.0001, suggesting some significance for these direct relationships.

The validity of the results on stress wave travel time by bacterial infection class was better in a full-size board than at a single analysis point, because both the sensing of

SW TRAVEL TIME ALONG THE BOARD LENGTH

Max SW Travel Distance, Clear Wood

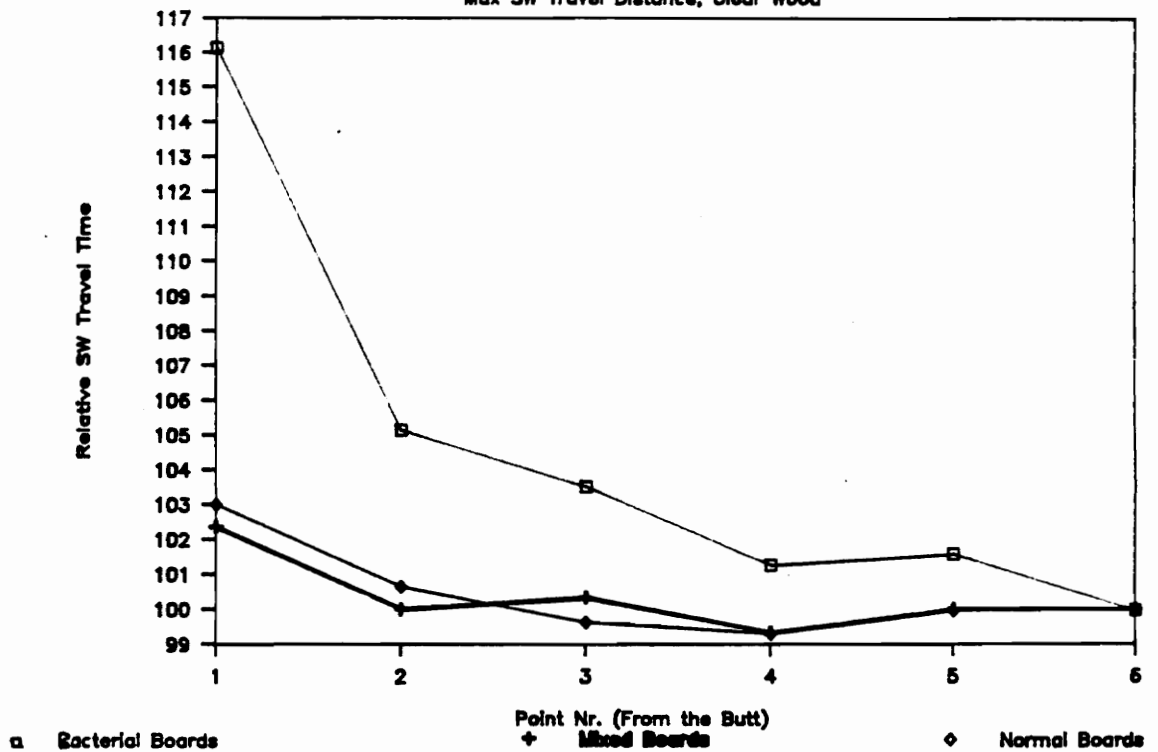


Fig. 8. Relative Stress Wave Travel Time along the Length of a Bacterial, Mixed and "Normal" Board. Reading Closest to the Top = 100.

SW TRAVEL TIME IN BUTT AND TOP BOARDS

Max SW Travel Distance, Clear Wood

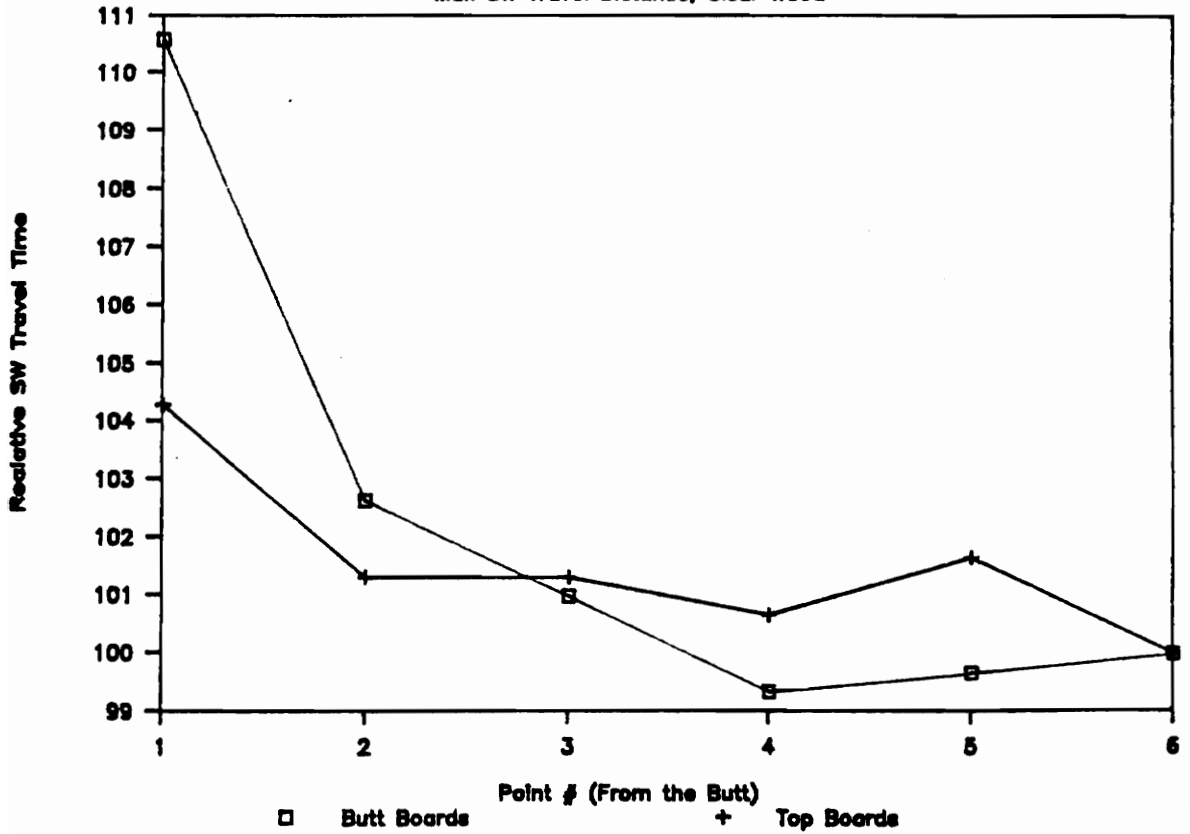


Fig. 9. Relative Stress Wave Travel Time along the Length of a Butt and Top Board. Reading Closest to the Top = 100.

bacterial infection and the computations for stress wave results for a board were based on several observations rather than one. Since the class intervals for the bacterial infection in a board were rather large (Chapter 521, p. 20) the possibility for an incorrect evaluation was reduced.

613. Effect of the Defects in Green Lumber to the
Identification of Bacterial Infection by Stress Wave
Travel Time

On average, the defects in green lumber had no significant effect on the stress wave travel time ($p = 0.6$), though it was longer, 344 usec/ft, at a point with a defect than at an adjacent clear point, 314 usec/ft. However, a separate analysis of the defects that could be expected to either increase or decrease stress wave travel time yielded some significant differences (Appendix 9).

Splits significantly ($p = 0.001$) increased the stress wave travel time. This was consistent with the results from prior research (Ross and Pellerin 1991b). The other discontinuities in wood structure, such as an incipient ring failure, knot and worm holes and pith did not have any significant effect ($p = 0.5$). Knots did not have any

significant effect ($p = 0.2$) when performing the stress wave analysis at the maximum possible travel distance. However, they significantly ($p = 0.01$) decreased the stress wave travel time when using the 4-inch travel distance. The decrease was attributable to their higher density and to the occurrence of cross-grain in their vicinity compared to a normal stem wood (Gerhards 1983, Hamm and Lum 1991). The effect of the stress wave travel distance was attributable to the less percentage of knot wood at a longer stress wave travel distance. Particularly the discontinuities but also the knots had a significantly greater effect to stress wave travel time at certainly infected points than at possibly mildly infected or uninfected points.

614. Capability, Interactions and Rank of the Predictors for Stress Wave Travel Time

Results of the correlation analysis on the possible predictors for stress wave travel time in a board and their interactions are shown in Appendix 10. Mean and maximum stress wave travel times had a direct relationship with the estimated percentage of bacterially infected wood of the board volume, the sensed worsening bacterial infection class and the measured moisture content, and an inverse

relationship with basic density, in particular.

Bacterial infection class and percentage bacterially infected volume were related to grain pattern: the more the grain pattern deviated from flat-sawn the more extended the infection was. Because stress wave travel time had a much stronger relationship with bacterial infection than grain pattern, the risk to sort boards by grain pattern instead of bacterial infection was small. Other relationships between the possible predictors were of no importance for the conclusions of the ability of stress wave travel time to identify bacterial boards.

The summaries of the stepwise procedures to predict the stress wave travel time are shown in Appendix 10. Percentage bacterially infected volume and moisture content proved out to be the primary predictors for mean and maximum stress wave travel time. Because moisture content was not significantly different in bacterial compared to other boards, there was the possibility that random variation in moisture content between single boards caused errors in separating bacterial and other boards by stress wave travel time. It remained an open question whether this suspicion was true, since no relationship was observed between stress

wave travel time and moisture content. Grain pattern and the location of a board along the length of a log had some importance. Much variation remained unexplained, as indicated by low R-Squares of the final models: 0.11 for the mean and 0.18 for the maximum stress wave travel time.

615. Efficiency of Separating Bacterial and "Normal" Boards by Stress Wave Travel Time

Maximum stress wave travel time appeared to be the most useful of the studied stress wave variables to identify bacterially infection in a board. Boards where the maximum stress wave travel time was beyond a specified limiting value were expected to be bacterial, and those where it was below the value were expected to be "normal".

If one wanted to isolate as much as 80 percent of the 93 bacterial boards, the limiting max stress wave travel time should be about 300 $\mu\text{sec}/\text{ft}$ but 60 percent of the 80 "normal" boards would be incorrectly identified. If one were content with isolating 40 percent of bacterial boards, the limiting value should be 350 $\mu\text{sec}/\text{ft}$ and only 15 percent of the "normal" boards would be incorrectly identified.

Considering the stress wave travel time on clear points only would have reduced the number of incorrectly identified "normal" boards by 4 and 2 percentage points, respectively. Assuming the percentage of bacterial boards in the charge of 10 percent, for example, the procedures using all observations in a board would then isolate 62 and 18 percent of the total number of boards, respectively.

The results with this sorting procedure were worse than those obtained by Ward et al. (1991). Using a limiting maximum stress wave travel time of 480 usec/ft they were able to correctly identify 98 percent of "normal" and 84 % of bacterial boards. In the data of my study, this limit would have correctly identified 90 percent of "normal" but only 20 percent of bacterial boards. This may be attributable to the difference in sampling which resulted in a difference in the structure of the data. Ward et al. (1991) most likely sampled very heavily infected stems, where the presence of bacterial infection was detected from increment cores already prior to felling. Very heavily infected stems typically have shake which considerably increases the stress wave travel time.

The identification of "normal" boards with the maximum

stress wave travel time in the study of Ward et al. (1991) was the more successful the better the grade was, and that of bacterial boards was the more successful the worse the grade was. This indicated that low-quality boards may be identified as bacterial because of the defects instead of the bacterial infection in itself. Concluded from the results of this study, this is possible only if the defects are splits, holes, decay, etc. which definitely increase the stress wave travel time. At least shake, frost cracks, and incipient ring failure are closely related to a severe bacterial infection in red oak wood, and thus facilitate the identification. On the other hand, end splits caused by timber cutting and storage can result to an incorrect identification of an uninfected board as infected. If the defects are knots the stress wave travel time should rather decrease.

When using the mean stress wave travel time in a board as an identification criterion, the efficiency was generally worse than when using the maximum stress wave travel time. This was evident when attempting to isolate a low percentage of bacterial boards, in particular. Compared to the use of maximum stress wave travel time, the percentages of incorrectly identified "normal" boards would have increased,

when trying to attain equal percentages of correctly identified bacterial boards. An attempt to isolate 80 and 40 percent of bacterial boards would have resulted in an incorrect isolation of 56 and 30 percent of "normal" boards. Assuming again the percentage bacterial boards of 10 percent, the procedures would have isolated 58 and 31 percent of the total number of boards in the charge, respectively.

62. Tensile Strength Perpendicular to Grain and Drying

Defects vs. Bacterial Infection and Stress Wave Travel Time

621. Tensile Strength vs. Bacterial Infection and Stress Wave Travel Time.

Detailed results on tensile strength perpendicular to grain, expressed as maximum tensile stress, are shown by bacterial infection class are in Appendix 11. Compared to the data for the actual determination of the relationship between stress wave travel time and bacterial infection, this data had a systematic sampling (Chapter 525, p. 40). This resulted in more distinguished classes of bacterial infection, less within-class-variation and more significant differences in

stress wave travel time.

Tensile strength in the certainly infected specimens was lower than in the possibly mildly infected and uninfected specimens (Table 8, p. 70). The difference was significant ($p = 0.0001$). The difference between the infected and uninfected specimens, 43 percent, was larger than in a prior study on Southern red oak, 24 percent (Hart et al. 1984).

Tensile strength varied greatly between the specimens, ranging from 9 to 976 psi. It was possible that there already existed unidentified small checks or incipient ring failures in the specimens, which could have caused increase in stress wave travel time. Tensile strength of possibly mildly infected and uninfected specimens did not differ much from the published value of green Northern red oak, 750 psi (Wood Handbook 1987). However, it was considerably higher than the published value of Southern red oak, 480 psi.

Failure along one or several parallel wood rays - which represents a true or close to a true tension failure (Bodig and Jayne 1982), and a normal failure pattern in sound red oak (Youngs 1957) - was the most common among the specimens (Table 9, p. 70). It was the definite failure pattern among

Table 8. Stress Wave Travel Time and Maximum Tensile Stress by Bacterial Infection Class.

Bacterial Infection Class	Stress Wave Travel Time usec/ft	Maximum Tensile Stress psi
Certain	338	440
Possibly Mild	295	711
No	289	772

Table 9. Failure Pattern Distribution of Certainly Infected, Possibly Mildly Infected and Uninfected Tensile Strength Test Specimens. Failure Patterns: 1 = Strictly along a Wood Ray, 2 = Through Several Parallel Wood Rays, 3 = Strictly along Early Wood - Late Wood Interface, 4 = Combination of 1 and 3.

Bacterial Infection Class	Failure Pattern				Total
	1	2	3 %	4	
Certain	63	10	14	13	100
Possibly Mild	78	11	3	8	100
No	76	19	0	5	100

possibly mildly infected and uninfected specimens. A low tensile strength in connection with this failure pattern may indicate a susceptibility to end, internal and surface checking during drying. Failure along an early wood - late wood interface, or a combined failure along that and a wood ray, both of which have a strong indication of a shear failure, were more common among certainly infected than other specimens. A low tensile strength in connection with this failure pattern may indicate a susceptibility to development or aggravation of ring failure during drying.

The proclivity of weaker wood to fail along an early wood - late wood interface in contrast to the tendency of stronger wood to fail along a wood ray was observed. Tensile strength of the specimens that failed along the early wood - late wood interface was only 326 psi compared to 628 psi for those that failed along a wood ray. Examples of the different failure patterns are shown in Fig. 10 (p. 73).

The inverse relationship between tensile strength perpendicular to grain and stress wave travel time is evidenced by Fig. 11 (p. 74). The increasing stress wave travel time sharply decreased the tensile strength until a limiting value after which the decrease was very slow. A

lower limiting value of 350 $\mu\text{sec}/\text{ft}$ for the weak specimens, and an upper limiting value of 280 $\mu\text{sec}/\text{ft}$ for the strong specimens were observed. The observations between these values could be considered as intermediate cases, however, with an excessively large variation in tensile strength. A simple linear regression analysis weighted with the variance yielded the following statistics for the relationship:

Constant (Y-Intercept)	1741.7
X-Coefficient (Slope)	-3.662
Standard Error of Y-Estimate	171.6
R-Square	0.616

Splitting the data by bacterial infection class showed the dominant influence of the certainly infected specimens on the overall regressions (Fig. 12, p. 75). An equal increase in stress wave travel time resulted in a less decrease in tensile strength among certainly infected than other specimens (X-Coefficient -3.0 vs. 5.3). However, the difference in R-Square was insignificant.

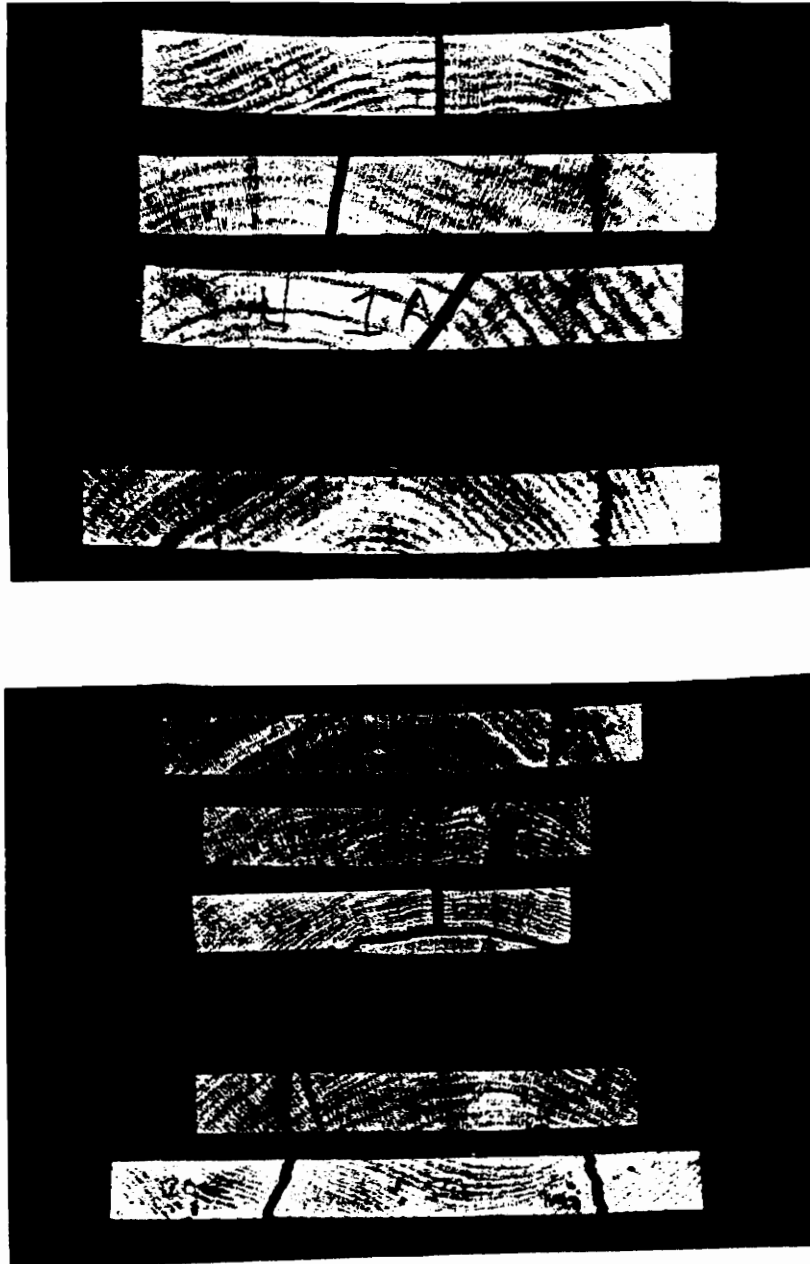


Fig. 10. Examples of the Different Failure Patterns in the Tensile Strength Tests Perpendicular to Grain.

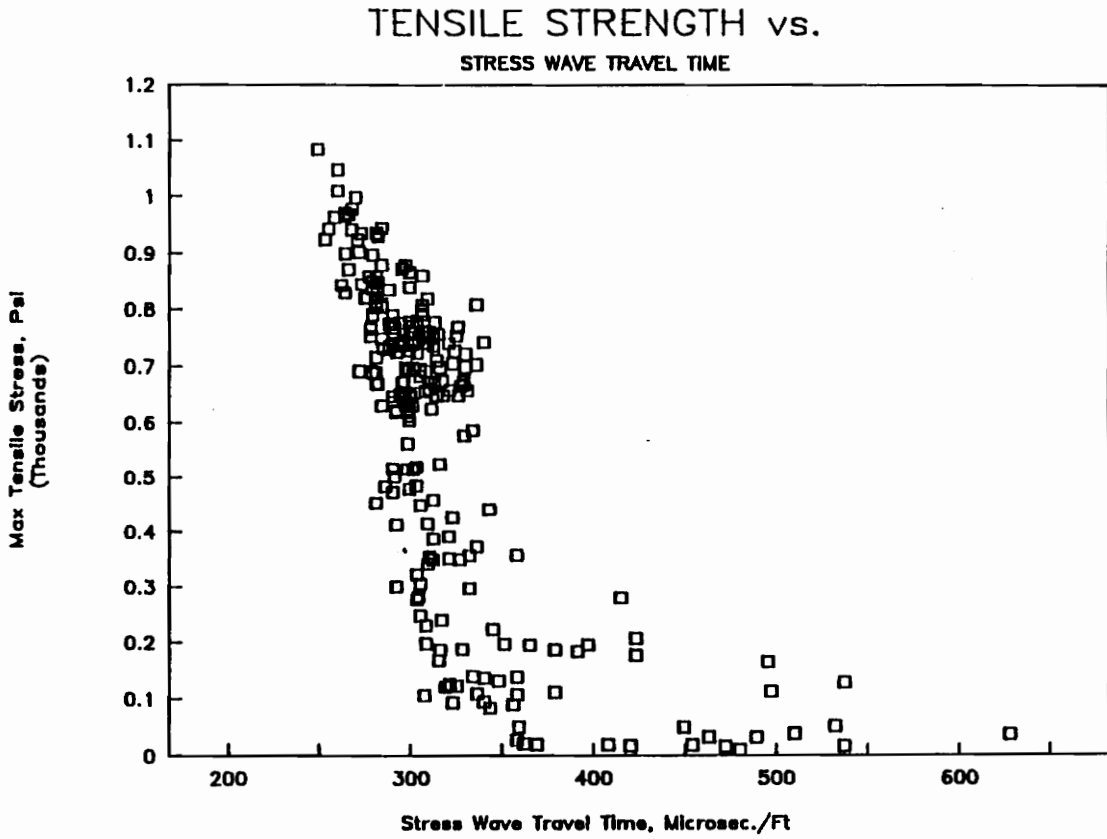


Fig. 11. Tensile Strength Perpendicular to Grain vs. Stress Wave Travel Time.

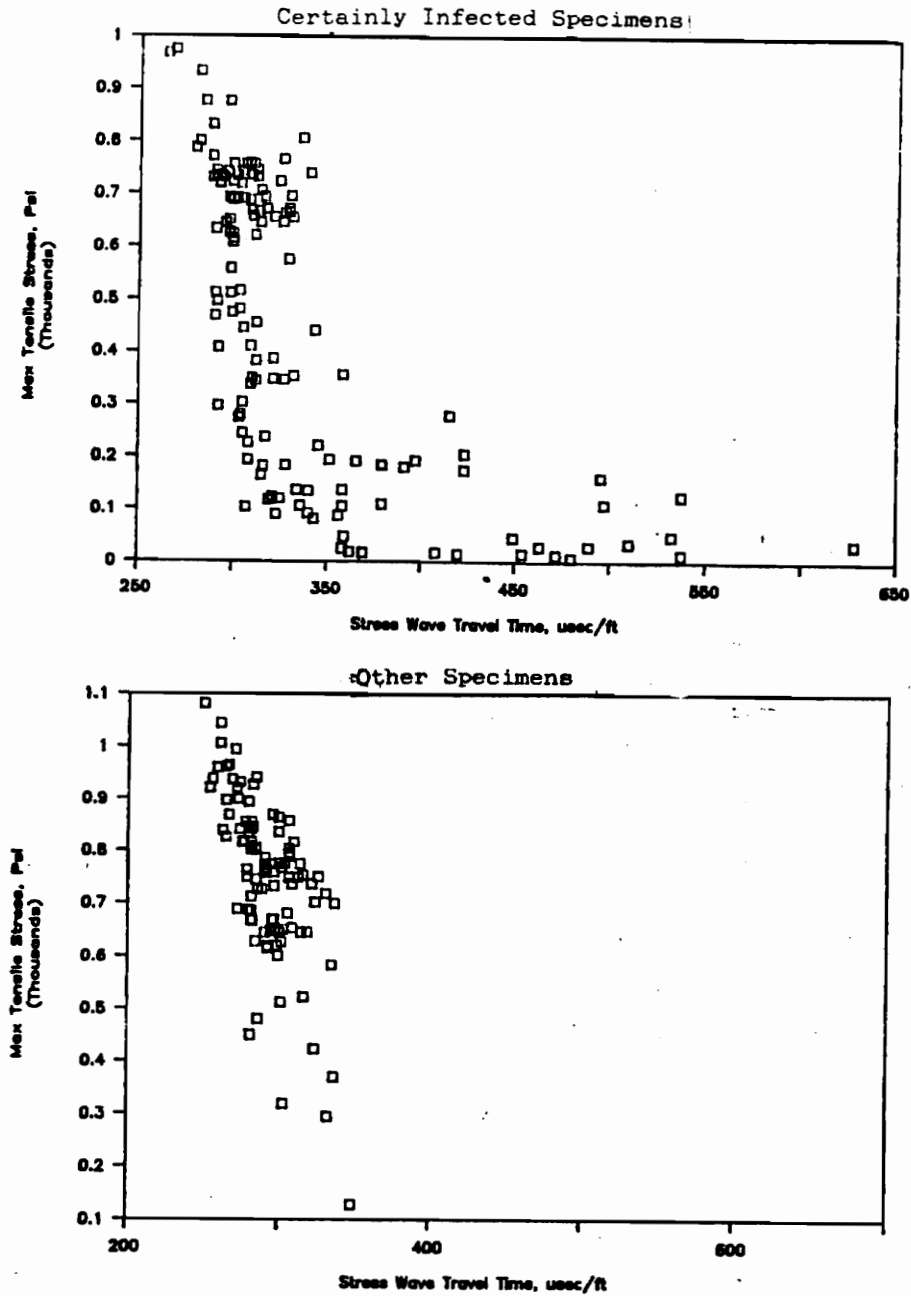


Fig. 12. Tensile Strength Perpendicular to Grain vs. Stress Wave Travel Time among Certainly Infected (Above), and Possibly Mildly Infected and Uninfected Specimens (Below).

Results of the correlation analysis on the possible predictors for tensile strength perpendicular to grain are shown in Appendix 12. Tensile strength had a strong inverse relationship with stress wave travel time, and a weaker inverse relationship with moisture content. Expected interactions existed between almost all possible predictor variables. Especially stress wave travel time had a strong inverse relationship with bacterial infection class.

The summary of the stepwise procedure to predict tensile strength is shown in Appendix 12. Stress wave travel time, green density and bacterial infection class were the apparent predictors, yielding an R-Square of 0.67.

622. Conditions in the Kiln-Drying Experiment

The designed and actual drying schedule, and the times for each step are shown in Table 10 (p. 77). The changes were made based on the moisture content of the wettest half of the sample boards. The fans were reversed every 6 hours.

The moisture content of the sample boards along with the dry-bulb and wet-bulb temperature is shown in Fig.13 (p. 79). Due to the high outside temperature, low wet-bulb

Table 10. The Designed (T4D2, Rasmussen 1961) and Actual Drying Schedule in the Kiln Drying Experiment. MC = Moisture Content, DBT = Dry-Bulb Temperature, WBT = Wet-Bulb Temperature, RH = Relative Humidity, EMC = Equilibrium Moisture Content.

MC %	Designed				Actual				Time for the Step Hours
	DBT °F	WBT °F	RH %	EMC %	DBT °F	WBT °F	RH %	EMC %	
>50	110	106	87	17.5	110	106	87	17.5	190.5
50	110	105	84	16.2	110	105	84	16.2	76.0
40	110	102	75	13.3	110	102	75	13.3	36.0
35	110	96	60	9.9	110	96	60	9.9	47.0
30	120	90	29	5.2	120	90	29	5.2	49.0
25	130	80	10	2.0	130	90	21	3.8	48.0
20	140	90	14	2.6	140	94	20	3.5	69.0
15	180	130	26	3.3	180	145	41	5.0	} 100.0
5	180	145	41	5.0	180	145	41	5.0	
6	180	145	41	5.0	180	157	57	7.0	23.0
7	Kiln Shut Down								

temperatures and subsequent high wet-bulb depressions could not always be achieved at the later stages of drying when the dry-bulb temperature was high. Drying rate during the first week clearly exceeded the maximum safe drying rate of 3 percent per day for 4/4 northern red oak lumber (Wengert 1990). The stage of equalizing was extended by raising the wet-bulb temperature to avoid shutting down the kiln during a weekend.

The drying conditions were more severe than provided by the schedule T4D2 in a commercial kiln. This was because in this experiment both sides of the (narrow) lumber stacks were all the time under drying while one side of the (wide) lumber stack in a commercial kiln is in rest while the other side is drying. This along with the small experimental material meant that the experiment was exploratory.

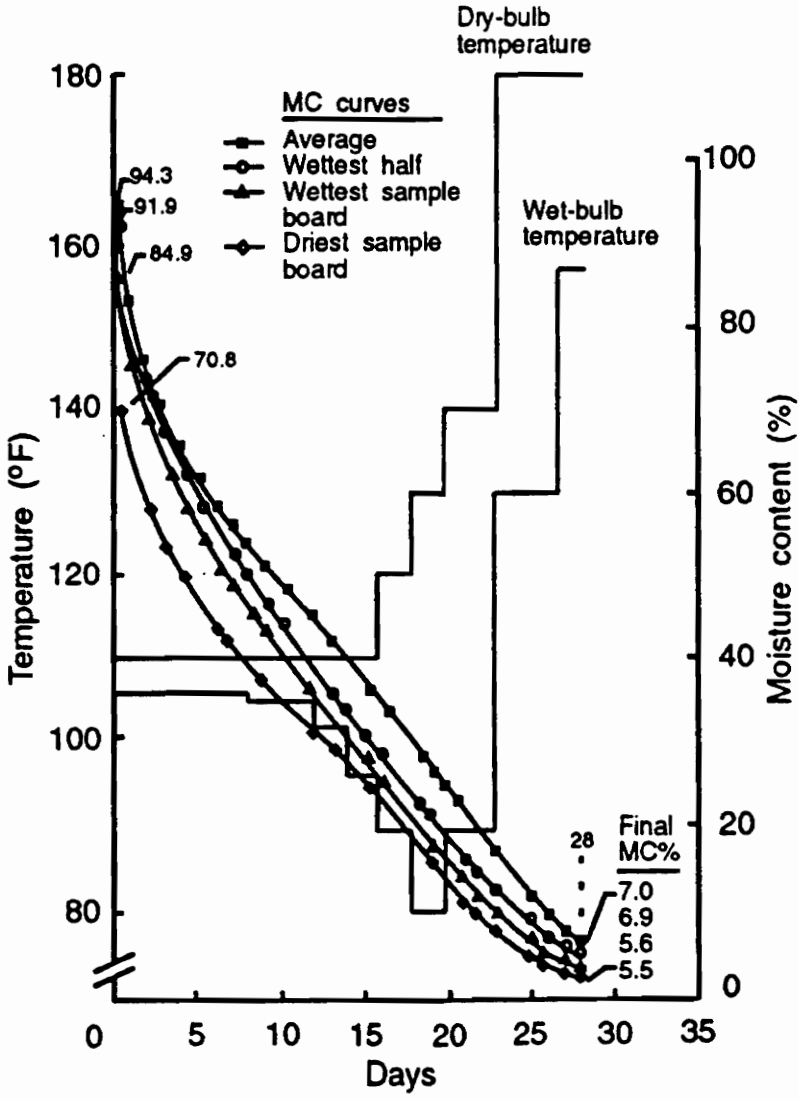


Fig. 13. Progress of Lumber Drying vs. Adjustments of Dry-Bulb and Wet-Bulb Temperature in the Kiln-Drying Experiment.

623. Drying Defects vs. Bacterial Infection

The stress wave travel time in the kiln-drying material was longer at certainly infected analysis points than at other points, and the difference was significant ($p = 0.0001$) but smaller than in the whole material (Table 11, p. 82). Again, no significant difference was observed between possibly mildly infected and uninfected points. Thus, the conclusions of the relationship stress wave travel time vs. bacterial infection based on the whole material could be generalized for the material of kiln-drying experiment as well.

Detailed results on drying defects at single clear analysis points in flat-sawn lumber are shown by bacterial infection class in Appendix 13. The drying defects whose development (honeycomb, surface checks) or aggravation (ring failure) should be typical for bacterially infected red oak occupied 40 percent of the certainly infected points, 22 percent of the possibly mildly infected points and 20 percent of the uninfected points. Especially ring failure and honeycomb were more frequent at certainly infected points. They had also more severe defects than other points.

As in the whole board material, the mean and maximum stress wave travel time was longer in kiln-dried bacterial boards than kiln-dried other boards, and the difference was significant ($p = 0.0001$) but smaller than in the whole material (Table 12, p. 82). Thus, the conclusions of the relationship stress wave travel time vs. bacterial infection in a board based on the whole board material could be generalized for the boards in the kiln-drying experiment as well.

Detailed results on the occurrence of each drying defect and its maximum severity in a flat-sawn board, by grouping the boards by bacterial infection class, are shown in Appendix 14. The percentages for the occurrence of defects were here double to triple compared to those at single analysis points. This indicated that the defects were concentrated to limited sections in boards. Of bacterial boards, 87 percent had either honeycomb, surface check, ring failure or end check or split in a clear wood, and 44 percent of them had a heavy defect. A defect was present in 57 percent of mixed boards and in 50 percent of "normal" boards, but the defects were here less severe than in bacterial boards. Especially ring failure and honeycomb were more frequent in bacterial than other boards.

Table 11. Stress Wave Travel Time at Clear, Flat-Sawn Analysis Points of the Material for Kiln-Drying Experiment by Bacterial Infection Class.

Bacterial Infection	Stress Wave Travel Time usec/ft
Certain	313
Possibly Mild	294
No	296

Table 12. Stress Wave Travel Time in Full-Size, Flat-Sawn Boards for the Kiln-Drying Experiment by Bacterial Infection Class.

Bacterial Infection Class of a Board	Stress Wave Travel Time usec/ft	
	Mean	Maximum
Bacterial	322	370
Mixed	295	310
"Normal"	299	319

Table 13. Percentage of the Board Volume Degraded During by Bacterial Infection Class.

Bacterial Infection Class of a Board	Mean Percentage Degraded
Bacterial	36
Mixed	18
"Normal"	13

The mean estimated percentage board volume degraded during drying, 22 percent, was high, and further indicated the more severe drying conditions than planned (Table 13, p. 82). For bacterial boards, it was more than double compared to mixed boards, and triple compared to "normal" boards.

The results of the relative differences between infected and uninfected boards matched well with those by Ward and Groom (1983), but the overall drying degrade was higher in this study.

No relationship was found between degrade percent and estimated percentage of bacterially infected wood in a board. The R-Square as low as 0.0136 showed that other factors than the estimated extent of bacterial infection were much more important for the drying degrade. On the other hand, the crude technique to estimate the degrade percent and the percentage bacterially infected wood was likely to result in a weaker correlation than it was actually.

624. Drying Defects vs. Stress Wave Travel Time

Detailed results on drying defects at a single stress wave analysis point in three classes of stress wave travel time are shown in Appendix 15. The class limits were established based on the results of tensile strength tests: the limiting values of 280 and 350 $\mu\text{sec}/\text{ft}$ for stress wave travel time were to separate points with a wood of high, intermediate and low tensile strength perpendicular to grain, and thus separate those with low, moderate and high risk to degrade during drying.

Of the clear points with a long stress wave travel time, 58 percent had a drying defect, compared to 21 and 18 percent, respectively, for the points with a moderate and short stress wave travel. Especially honeycomb and ring failure were much more common in the first category. The difference in the frequency of drying defects was more significant between the three stress wave travel time classes than between the bacterial infection classes.

Detailed results on the occurrence of each drying defect with its maximum severity in a board, by grouping the boards by the maximum stress wave travel time observed, are shown

in Appendix 16. Compared to the results on single analysis points, the degrade frequency was here 1.5 to 3 times higher. Of the flat-sawn boards with a long maximum stress wave travel time, 95 percent had a drying defect, while the corresponding figures for the boards with a moderate and short stress wave travel time were 60 and 47 percent, respectively. The largest differences existed in honeycomb, ring failure and butt splits. Observable differences were between the boards with a moderate and low maximum stress wave travel time, as well. As for single analysis points, the difference in the susceptibility to degrade was larger in the comparison of stress wave travel time classes than in the comparison of the bacterial infection classes.

The mean percentage board volume degraded during drying was threefold for flat-sawn boards with a long maximum stress wave travel time compared to those with a moderate, and eightfold compared to those with a short maximum stress wave travel time (Table 14, p. 86). The relative differences between the three categories remained at similar level when using classification by mean stress wave travel time. However the separation of defect-prone boards was more inefficient judged by the decreased percentage for the category with a long stress wave travel time.

Table 14. Percentage of the Board Volume Degraded During
Drying by Stress Wave Travel Time Class.

Stress Wave Travel Time, usec/ft	Maximum in a Board	Mean in a Board
	Mean Degrade Percent	
> 350	60	50
280-350	24	17
< 280	11	6

Fig. 14 (p. 88) shows the distribution of flat-sawn boards to the different categories of degrade percent in the three aforementioned classes of maximum stress wave travel time. All boards with a long maximum stress wave travel time degraded during drying, and 60 percent of them had a degrade percent more than 60 percent. Boards with a short maximum stress wave travel time degraded slightly at their most severe, and 70 percent of them developed no degrade. Fig. 15 (p. 89) illustrates the visual differences in drying degrade between the boards with a long and short maximum stress wave travel time.

No actual relationship was found between degrade percent and the maximum and mean stress wave travel time in a board, though the simple linear regression analyses showed positive slopes: R-Squares were 0.28 and 0.18, respectively. The maximum stress wave travel time as a predictor yielded the steeper slope as well. The crude technique to estimate the degrade percent was likely to result in weaker correlations than they were actually.

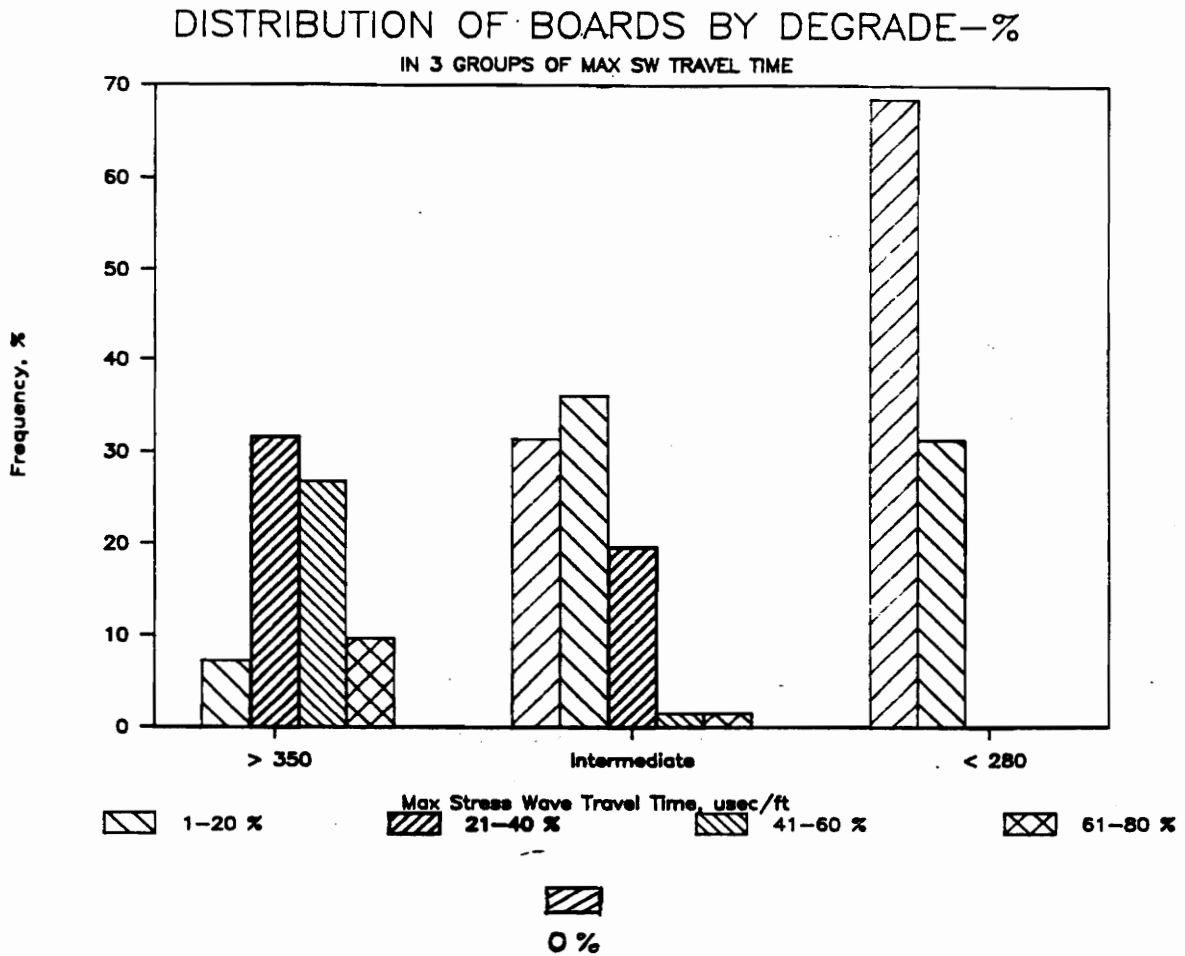


Fig. 14. Distribution of Flat-Sawn Boards to Different Categories of Percentage Board Volume Degraded During Drying in the Categories of Maximum Stress Wave Travel Time of Less than 280 usec/ft, 280 to 350 usec/ft and More than 350 usec/ft.

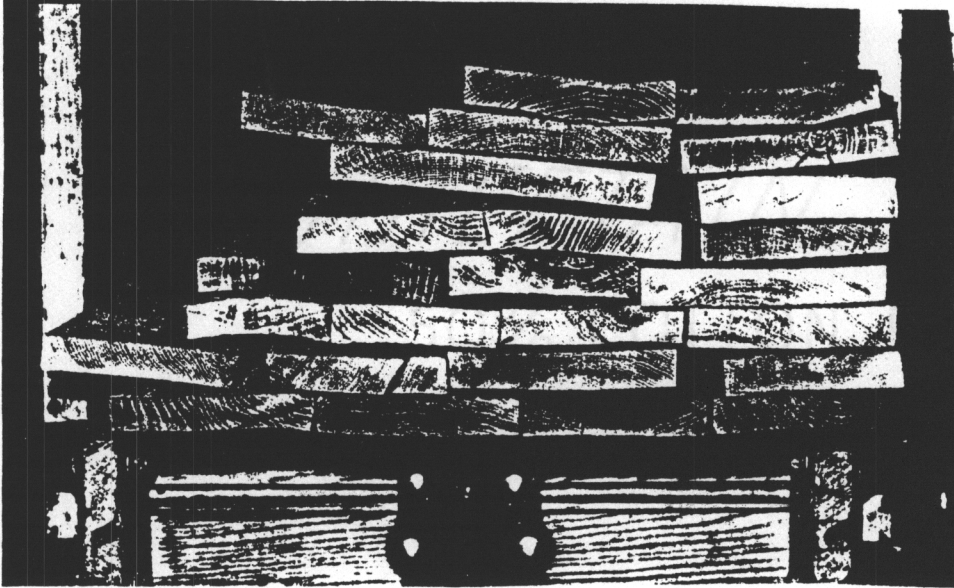


Fig. 15. Boards with the Maximum Stress Wave Travel Time More than 350 usec/ft (Above) and Less than 280 usec/ft (Below) after Drying, the Butts Facing.

625. Capability, Interactions and Rank of the Predictors for Drying Defects

Results from the correlation analysis on the possible predictors for degrade percent in a board are shown in Appendix 17. Drying degrade had a very strong direct relationship with stress wave travel time variables, and a rather strong relationship with percentage bacterially infected volume in board, sawing pattern more close to quarter-sawn than flat-sawn, board width and moisture content. Some inverse relationship existed between drying degrade and basic density. The results were consistent with the current knowledge of the crucial wood properties for the quality of oak drying (Wengert 1990).

The summaries of the stepwise procedures to predict the degrade percent are shown in Appendix 17. The maximum stress wave travel time proved to be a definite predictor. The bacterial infection class of a board, but also the grain pattern and board width had additional significance. The overall R-Square value for the final regression model, 0.44, indicated a high degree of variation not accounted for.

7. CONCLUSIONS

7.1. Stress Wave Travel Time vs. Bacterial Infection

The limiting factor for evaluating the results of this study was the uncertainty in establishing the presence of bacterial infection by odor and discoloration. Even though an estimate could be obtained of the extent of bacterial infection in a piece of lumber, it was an uncertain way to evaluate the presence of infection at a particular spot.

The verification of the sensed bacterial infection by scanning electron microscopy (SEM) did not provide any generalization for a full-size board. On the other hand, it did not show any distinct errors in sensing either. However, sensing by odor and discoloration was not capable to distinguish a mild infection from no infection.

A strong relationship was found between the stress wave travel time across the grain of green, clear red oak lumber and the degree of bacterial infection: the certain infection increased the relative stress wave travel time, though the absolute difference was not large. In a full-size board, a heavy bacterial infection was identified more efficiently by

the maximum instead of the mean stress wave travel time, suggesting that individual high stress wave travel times may be essential for the identification. That is why, several observations along the full length of the board are needed for a proper identification. Stress wave analysis across as full a board width as possible proved out to be as reliable as and technically more feasible than that at a short constant distance in sections where the grain pattern was the most uniform.

Considering all observations along the length of the board, instead of those at clear points only, may have a significant effect on the maximum stress wave travel time observed, if the board has splits, holes or decay. If all observations are used, an incorrect identification of an uninfected board as infected may occur, but an opposite error is not expected. The knots do not affect the identification because the decreased stress wave travel time makes it easier for the higher stress wave travel time caused by the infection to show up. Knots appeared to be more common in infected than uninfected boards, thus theoretically resulting in an incorrect identification of a mildly infected board as uninfected. Analyzing larger data the errors attributable to defects become fewer or may

totally disappear.

Considering moisture content along with the stress wave travel time did not facilitate the identification of bacterial boards, neither did its variation hamper the stress wave analysis in green lumber. Moisture content in itself did not provide any means to evaluate the severity of infection.

Because of the overlapping of stress wave travel time in infected and uninfected boards, a certain amount of incorrectly sorted boards cannot be avoided if the method is applied to practical working conditions. If only the worst infected boards need to be isolated, this problem is reduced.

72. Tensile Strength and Drying Defects vs. Bacterial Infection and Stress Wave Travel Time

A strikingly low tensile strength perpendicular to grain in bacterially infected red oak wood strongly indicated a high susceptibility to check during drying. Because decreased tensile strength was indicated by increased stress wave travel time typical for infected wood, stress wave analysis

was able to indicate possibility of drying degrade.

Failure pattern in the tensile strength tests was also associated with bacterial infection and stress wave travel time. A frequent failure of infected wood along early wood - late wood interface indicated susceptibility to develop or aggravate ring failure during drying. In contrast, the predominant failure of uninfected wood along a wood ray rather indicated a proclivity to checking and honeycombing (in a radial direction).

The results on the average level of drying defects cannot be generalized for commercial kiln operations. Relative differences between lumber classes should still be valid. In addition, the results cannot be directly generalized for the whole red oak group because of the between-species-variation in wood properties, and because the boards used could not be identified as to species.

As expected from the tensile strength tests, bacterially infected red oak lumber degraded considerably more during drying than uninfected lumber. Especially ring failure, honeycomb, and butt checks and splits were more frequent in infected than uninfected lumber. The defects were more

severe in infected lumber as well.

Lumber with a long stress wave travel time developed considerably more defects than lumber with a short stress wave travel time. As consistent with the conclusions from the relationship between bacterial infection and stress wave travel time, the maximum stress wave travel time of several observations in a board identified the defect-prone boards more efficiently than the mean stress wave travel time.

8. SUMMARY

A sample of 241 green 4/4 red oak boards from Southcentral Virginia was analyzed by stress wave timing in the width direction at several points along the length to establish the relationship between bacterial infection and stress wave travel time. Bacterially infected red oak lumber is expected to develop more surface, internal and end checks, and develop or aggravate ring failure during drying than uninfected lumber.

Because tensile strength perpendicular to grain is inversely related to the tendency for red oak lumber to check during drying, 244 small clear specimens were tested to establish the relationship of tensile strength to stress wave travel time in bacterially infected and uninfected wood. In addition, an exploratory kiln-drying experiment following a standard schedule (T4D2) was performed on 201 boards to study the actual relationship between drying defects and stress wave travel time.

The limiting factor for evaluating the results was the uncertainty in establishing the presence of bacterial infection by odor and discoloration. The verification by scanning electron microscopy (SEM) did not provide any

generalization for a full-size board. On the other hand, it did not show any distinct errors either. Sensing by odor and discoloration was incapable for identifying a mild infection.

Clearly identified bacterial infection increased the stress wave travel time across the grain at a single clear analysis point by 25 $\mu\text{sec}/\text{ft}$ (8 %) compared to possibly mild or no infection. No difference was detectable between possibly mildly infected and uninfected points. Similar trends were observed in full-size boards. The maximum stress wave travel time was 60 $\mu\text{sec}/\text{ft}$ (19 %) longer in boards sensed as bacterial (more than 70 % infected) than in other boards. The absolute difference in mean stress wave travel time was smaller. Stress wave analysis across the full width of lumber yielded a clearer difference than that at a short constant distance in the most flat-sawn section.

Stress wave analysis at points at a constant distance from each other along the length of the board yielded a better identification of bacterial boards than that at clear points only, because the defects increasing the stress wave travel time (splits, incipient ring failure, knot and worm holes) were more frequent in bacterial than other boards. Knots

decreased the stress wave travel time. but they did not generally hinder the identification of bacterial boards by stress wave timing.

Considering moisture content along with the stress wave travel time did not facilitate the identification of bacterial boards; neither did its variation hamper the stress wave analysis in green lumber. Moisture content in itself did not provide any means to evaluate the severity of infection.

Stress wave travel time was able to separate the boards sensed as most severely infected but a considerable uncertainty existed for the intermediate boards. Thus, a certain amount of incorrectly separated uninfected boards cannot be avoided if the technique is applied to practical conditions. Their amount was reasonable if one wanted to separate only the most severely infected boards.

Tensile strength perpendicular to grain averaged 43 percent lower in clearly infected than uninfected wood. Increased stress wave travel time also indicated decreased tensile strength. Infected wood with a long stress wave travel time commonly failed along the early wood - late wood interface,

which may indicate susceptibility to develop or aggravate ring failure during drying. Mildly infected and uninfected wood failed predominantly along a wood ray, which is the failure plane in surface checking and honeycombing.

Stress wave analysis points sensed as clearly infected and boards sensed as bacterial developed considerably more drying defects than other points and boards, respectively. The defects in infected lumber were also more severe than in uninfected lumber. Lumber with a long stress wave travel time, which was expected to be weak in tensile strength, developed considerably more defects than lumber with short stress wave travel time, which was expected to be strong.

LITERATURE CITED

- Bertholf, L.F. 1965. Use of Elementary Stress Wave Theory for Prediction of Dynamic Strain in Wood. Washington State University, College of Engineering Bulletin 29. Pullman, Washington.
- Bodig, J. and B.J. Jayne. 1982. Mechanics of Wood and Wood Composites. Van Nostrand Reinhold Company. New York - Cincinnati - Toronto - London - Melbourne. 712 p.
- Gerhards, C.C. 1981. Effect of Cross Grain on Stress Waves in Lumber. USDA Forest Service Research Paper FPL-368. Forest Products Laboratory, Madison, Wisconsin.
- Gerhards, C.C. 1983. Effect of Knots on Stress Waves in Lumber. USDA Forest Service Research Paper FPL-384. Forest Products Laboratory, Madison, Wisconsin.
- Hamm, E. and C. Lum. 1991. Application of Ultra-Sonic Stress Waves to Detection of Compression Wood in Lumber. In: Proceedings, 8th International Nondestructive Testing of Wood Symposium, Vancouver, Washington (In Press). Washington State University, Pullman, Washington.
- Hart, C.A., R.C. Gilmore and J.C. Ward. 1984. Strength, Permeability, and Honeycomb in Bacterially-Infected Southern Red Oak. Unpublished Paper No. 1904 of the Journal Series of the North Carolina Agricultural Research Service, Raleigh, North Carolina 27695-7643. Paper presented at 38th Annual Meeting of the Forest Products Research Society, June 27, 1984, St. Louis, Missouri.
- Jayne, B.A. 1959. Vibrational Properties of Wood as Indices of Quality. Forest Products Journal 9(11): 413-416.
- Kaiserlik, J.H. 1975. Attenuation of Stress Waves as an Indicator of Lumber Strength. M.S. Thesis. Washington State University, Pullman, Washington.
- Kaiserlik, J.H. and R.F. Pellerin. 1977. Stress Wave Attenuation as an Indicator of Lumber Strength. Forest Products Journal 27(6): 39-43.
- Kersavage, P. 1988. Unpublished Data. Penn State University, State College, Pennsylvania.
- Kretschman, D. 1991. Personal Communication. U.S. Forest Products Laboratory, Madison, Wisconsin.
- Kutscha, N.P. and R.L. Ethington. 1962. Shelling Failures. Forest Products Journal 12(11): 538.

- Lawrence, A.H. 1991. Detection of Bacterially-Infected Red Oak by Ion Mobility Spectrometry. National Research Council of Canada, Institute for Aerospace Research. Laboratory Technical Report LTR-AA-1. 12 p. + Appendices, Ottawa, Canada.
- McGinnes, E.A., Jr., J.E. Phelps and J.C. Ward. 1974. Ultrastructure Observations of Tangential Shake Formations in Hardwoods. *Wood Science* 6(3): 206-211.
- NHLA. 1990. Hardwood Lumber Grading Rules. National Hardwood Lumber Association, Memphis, Tennessee.
- O'Halloran, M.R. 1969. Nondestructive Testing Parameters for Lodgepole Pine Dimension Lumber. M.S. Thesis. Colorado State University, Fort Collins, Colorado.
- Pellerin, R.F. 1965. A Vibrational Approach to Nondestructive Testing of Structural Lumber. *Forest Products Journal* 15(3): 93-102.
- Rasmussen, E. 1961. Dry Kiln Operator's Manual. USDA Forest Service Agriculture Handbook No. 188. Forest Products Laboratory, Madison, Wisconsin. 197 p.
- Ross, R.J. 1985. Stress Wave Propagation in Wood Products. Proceedings of the Fifth Nondestructive Testing of Wood Symposium. Washington State University, Pullman, Washington.
- Ross, R.J. 1991. Personal Communication. U.S. Forest Products Laboratory, Madison, Wisconsin.
- Ross, R.J. and R.F. Pellerin. 1991a. NDE of Green Material with Stress Waves: Preliminary Results Using Dimension Lumber. *Forest Products Journal* 41(6): 57-59.
- Ross, R.J. and R.F. Pellerin. 1991b. Nondestructive Testing for Assessing Wood Members in Structures: A Review. USDA Forest Service. General Technical Report FPL-GTR-70. Forest Products Laboratory, Madison, Wisconsin. 27 p.
- Sachs, I.B., J.C. Ward and R.E. Kinney. 1974. Scanning Electron Microscopy of Bacterial Wetwood and Normal Heartwood in Poplar Trees. Proceedings of the Workshop on Scanning Electron Microscopic Plant Science. I.I.T. Research Institute, Chicago., pp. 453-459.
- Schink, B., J.C. Ward and J.G. Zeikus. 1981a. Microbiology of Wetwood: Role of Anaerobic Bacteria Populations in Living Trees. *Journal of General Microbiology* 123: 313-322.
- Schink, B., J.C. Ward and J.G. Zeikus. 1981b. Microbiology of Wetwood: Importance of Pectin Degradation and *Clostridium* Species in Living Trees. *Applied Environmental Microbiology* 42: 526-532.

- Schink, B. and J.C. Ward. 1984. Microaerobic and Anaerobic Bacterial Activities Involved in Formation of Wetwood and Discolored Wood. IAWA Bulletin Vol.5(2): 105-109.
- Smulski, S. 1989. Relationship of Stress Wave and Static Bending-Determined Properties of Four Northeastern Hardwoods. In: Proceedings of Seventh International Nondestructive Testing of Wood Symposium, Washington State University, Pullman, WA, p. 301.
- Steel, R.G.D. and J.H. Torrie. 1980. Principles and Procedures of Statistics. A Biometrical Approach. Second Edition. McGraw-Hill Book Company. 633 p.
- Tanaka, T., H. Nagao and T. Nakai. 1991. Nondestructive Evaluation of Bending and Tensile Strength by Longitudinal and Transverse Vibration in Lumber. In: Proceedings of Eighth International Nondestructive Testing of Wood Symposium, Vancouver, WA (In Print). Washington State University, Pullman, Washington.
- Ward, J.C. 1978. Honeycomb: Dry Kiln or Bacteria. Abstracts of 32nd Annual Meeting of Forest Products Research Society, p. 30. Madison, Wisconsin.
- Ward, J.C. 1991. Personal Communication. USDA Forest Service, Forest Products Laboratory. One Gifford Pinchot Drive. Madison, Wisconsin.
- Ward, J.C. and D. Groom. 1983. Bacterial Oak: Drying Problems. Forest Products Journal 33(10): 57-65.
- Ward, J.C. and C.A. Hart. 1985. Drying North American Oak Lumber. In: Proceedings of North American Wood Drying Symposium; 1984 Nov. 27-28. Mississippi Forest Products Utilization Laboratory, Mississippi State, Mississippi.
- Ward, J.C., J.E. Kuntz and E. McCoy. 1968. Bacteria Associated with "Shake" in Broadleaf Trees. (Abstract) Phytopathology 59(8): 1056.
- Ward, J.C., P.L. Plantinga and C.J. Kozlik. 1989. Evaluation of Electronic Measurements for Presorting Hem-Fir Dimension Lumber. Unpublished Manuscript. U.S. Forest Products Laboratory, Madison, Wisconsin. 15 p.
- Ward, J.C. and W.Y. Pong. 1980. Wetwood in Trees: A Timber Resource Problem. USDA Forest Service General Technical Report PNW-112. Pacific Northwest Forest and Range Experiment Station. Portland, Oregon.
- Ward, J.C. and R.J. Ross. 1989. Exploratory Use of Stress Wave Analysis to Solve Drying Problems with Wetwood in Oak Lumber. Unpublished Study Plan. USDA Forest Service, Forest Products Laboratory, Madison, Wisconsin.

- Ward, J.C., R.J. Ross and A. TenWolde. 1991. Stress Wave Non-Destructive Evaluation for Identifying Oak Lumber with Bacterial Wetwood. Unpublished Manuscript. U.S. Forest Products Laboratory, Madison, Wisconsin. 13 p.
- Ward, J.C. and W.T. Simpson. 1987. Comparison of Four Methods for Drying Bacterially Infected and Normal Thick Red Oak. *Forest Products Journal* 37(11/12): 15-22.
- Ward, J.C. and D. Shedd. 1979. Californian Black Oak Drying Problems and the Bacterial Factor. USDA Forest Service Research Paper FPL 344. Forest Products Laboratory, Madison, Wisconsin.
- Ward, J.C. and J.G. Zeikus. 1980. Bacteriological, Chemical and Physical Properties of Wetwood in Living trees. In: Bauch, J.(Ed.). *Natural Variations of Wood Properties*. Mitteilungen der Bundesforschungsanstalt fur Forst- und Holzwirtschaft Nr. 131, pp. 133-166. Hamburg-Reinbek. Max Wiedehusen Verlag.
- Wengert, E.M. 1990. Drying Oak Lumber. Department of Forestry, University of Wisconsin-Madison, Madison, Wisconsin. 167 p.
- Wood Handbook. 1987. USDA Forest Service. Agriculture Handbook 72. Washington, D.C.. 466 p.
- Youngs, R.L. 1957. The Perpendicular-to-Grain Mechanical Properties of Red Oak as Related to Temperature, Moisture Content, and Time. USDA Forest Service, Forest Products Laboratory Report No. 2079. Madison, Wisconsin.
- Zinkel, D.F., J.C. Ward and B.F. Kukachka. 1969. Odor Problems from Some Plywoods. *Forest Products Journal* 19(12): 60.

Appendix 1. Listing of Codes for Board Defect Information.

A. Natural Defects

K = Knot.

KL = Large knot, greater than 1.0 inch diameter.

KM = Medium knot, 0.25 to 1.0 inch diameter.

KS = Small knot, less than 0.25 inch diameter, pin knots.

H = Hole.

HK = Knot holes, loose knots, etc.

HW = Large worm holes, ant galleries, decay holes.

HP = Pin holes, tiny worm holes.

B = Bark Pockets (Included bark with, or without, callus, pin knots, etc.)

BL = Large, width greater than 1 inch.

BM = Medium, width 0.25 to 1.0 inch.

BS = Small, width less than 0.25 inch.

W = Wane (greater than 25 percent of thickness).

P = Pith.

S = Splits, radial separations, or shake.

RF = Ring failure, ring shake or shelling.

D = Discoloration or mineral.

F = Fungal Action

Appendix 1. (Continued)

B. Drying Defects

Honeycomb:

- 1 = Light, in less than 20 percent of cross-section.
- 2 = Medium, in less than 50 percent of cross-section.
- 3 = Heavy, in more than 50 percent of cross-section.

Surface Checks and Splits:

- 1 = Light, in less than 10 percent of surface width.
- 2 = Medium, in less than 30 percent of surface width.
- 3 = Heavy, in more than 30 percent of surface width.

Ring Failure:

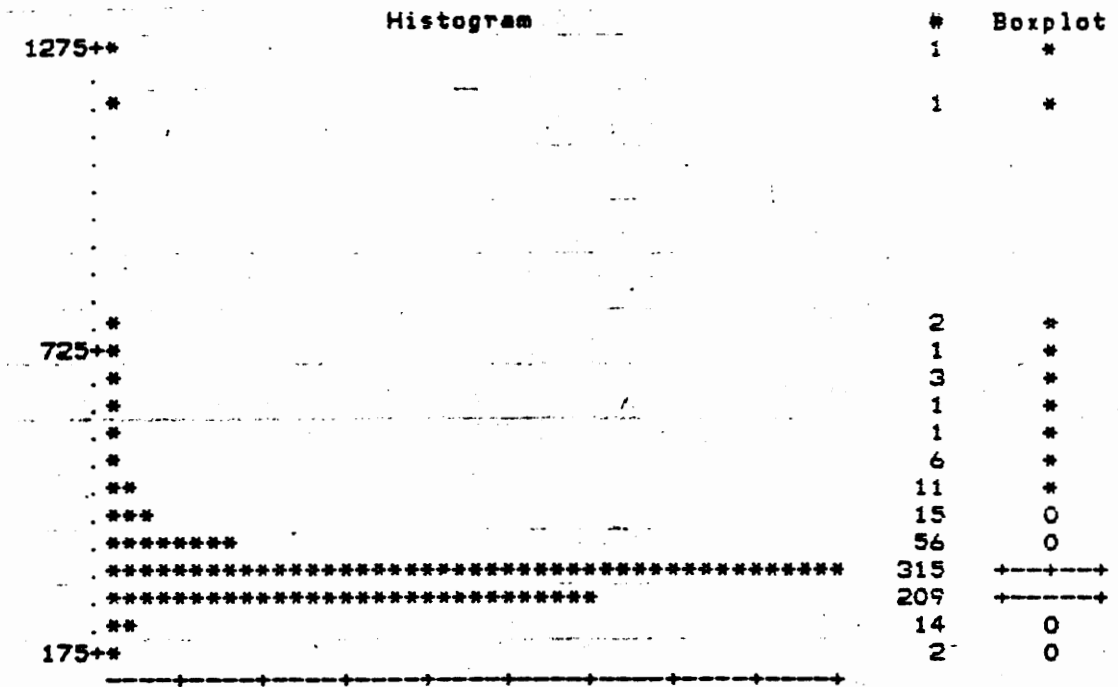
- 1 = Single separation near board surface.
- 2 = Single separation throughout the board
cross-section.
- 3 = Multiple separations.

End Checks and Splits:

- 1 = Light, in less than 20 percent of cross-section.
- 2 = Medium, in less than 50 percent of cross-section.
- 3 = Heavy, in more than 50 percent of cross-section.

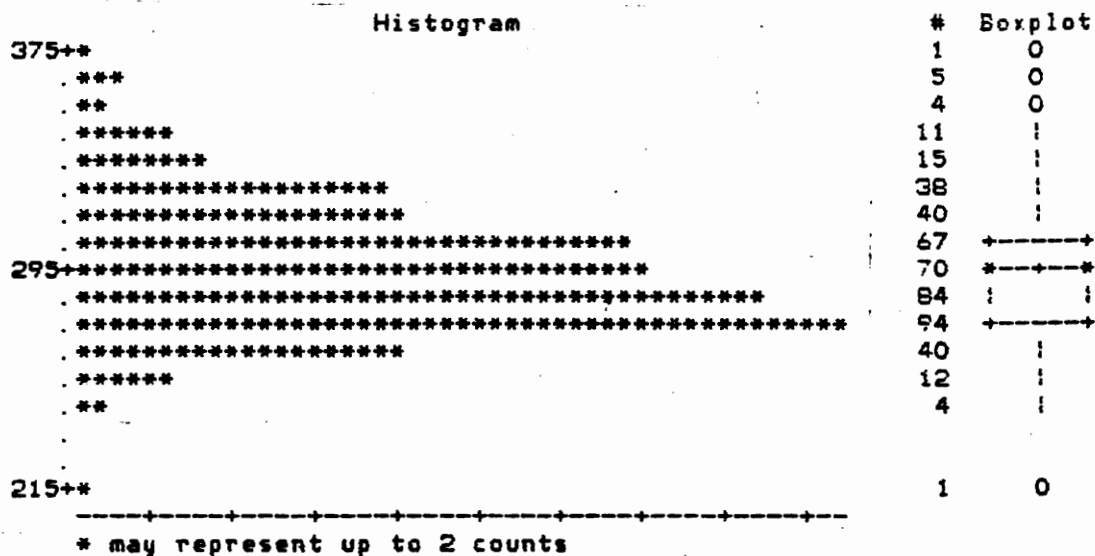
Appendix 2. Distribution of Stress Wave Travel Time Among Certainly Infected, Possibly mildly Infected and Uninfected Analysis Points.

1. Certainly Infected Points:



Appendix 2. (Continued)

2. Possibly Mildly Infected Points:



Appendix 3. (Continued)

2. Mixed Boards:

Mean Stress Wave Travel Time

Stem Leaf	#	Boxplot
39 6	1	0
38		
37		
36 1	1	0
35		
34 0447	4	:
33 11222	5	:
32		:
31 0236799	7	+-----+
30 00122256779	11	-----
29 0013445899	10	*-----*
28 01112234467889	14	+-----+
27 034788	6	:
26 456788	6	:
25 5	1	:
24 1	1	:
23		
22		
21 2	1	0

-----+
 Multiply Stem.Leaf by 10***+1

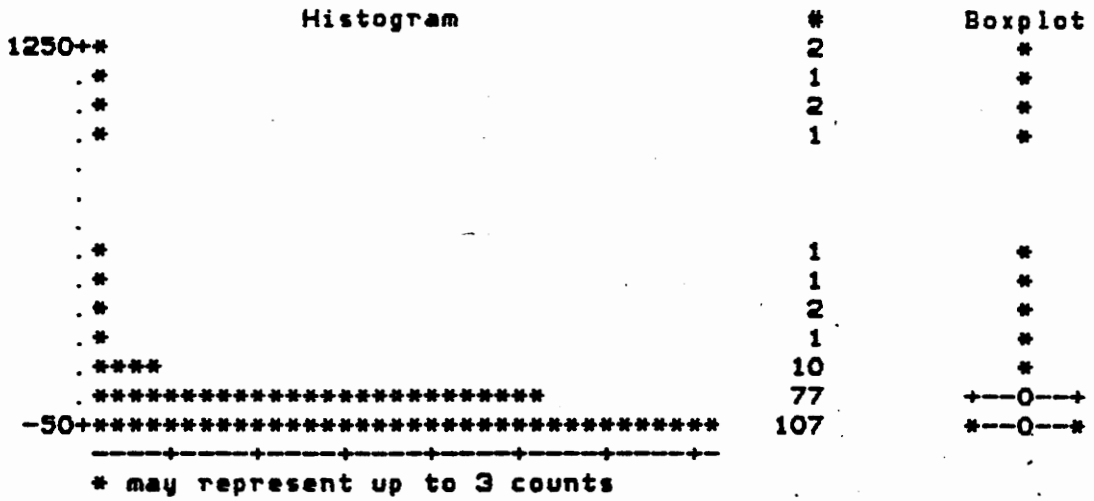
Maximum Stress Wave Travel Time

Stem Leaf	#	Boxplot
48 4	1	*
46		
44 4	1	*
42 3	1	0
40		
38 4	1	:
36 279	3	:
34 5788359	7	:
32 44590369	8	+-----+
30 12333455669922235599	20	*-----*
28 144566011444445777	18	+-----+
26 403579	6	:
24 9	1	:
22 0	1	0

-----+
 Multiply Stem.Leaf by 10***+1

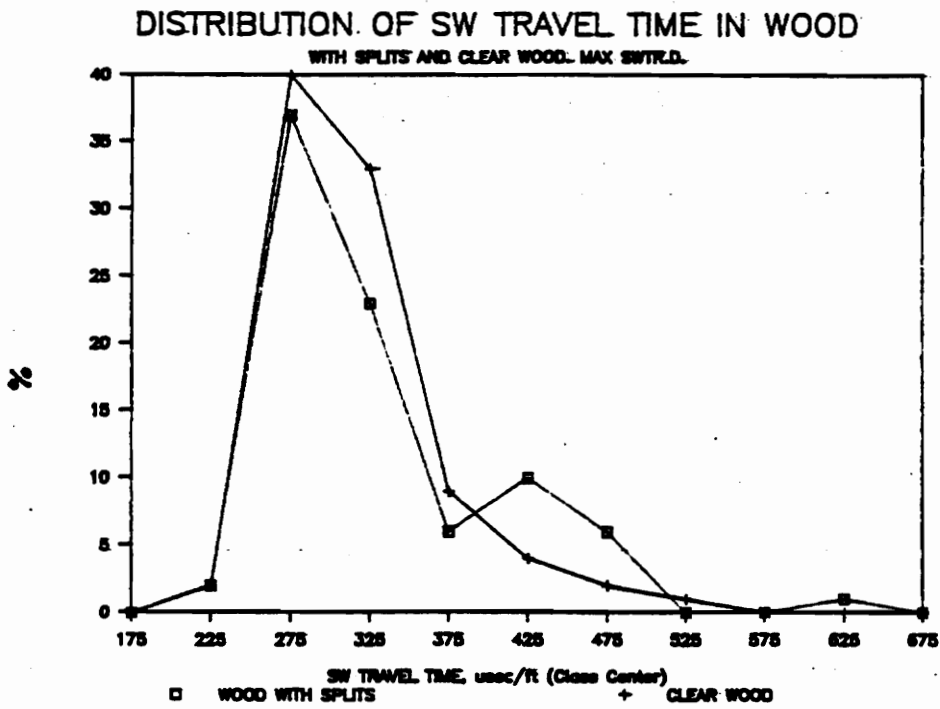
Appendix 4. Distribution of Stress Wave Travel Time Among Points with a Defect and Adjacent Clear Points, in a Green Condition.

1. Difference Considering All Possible Defects:



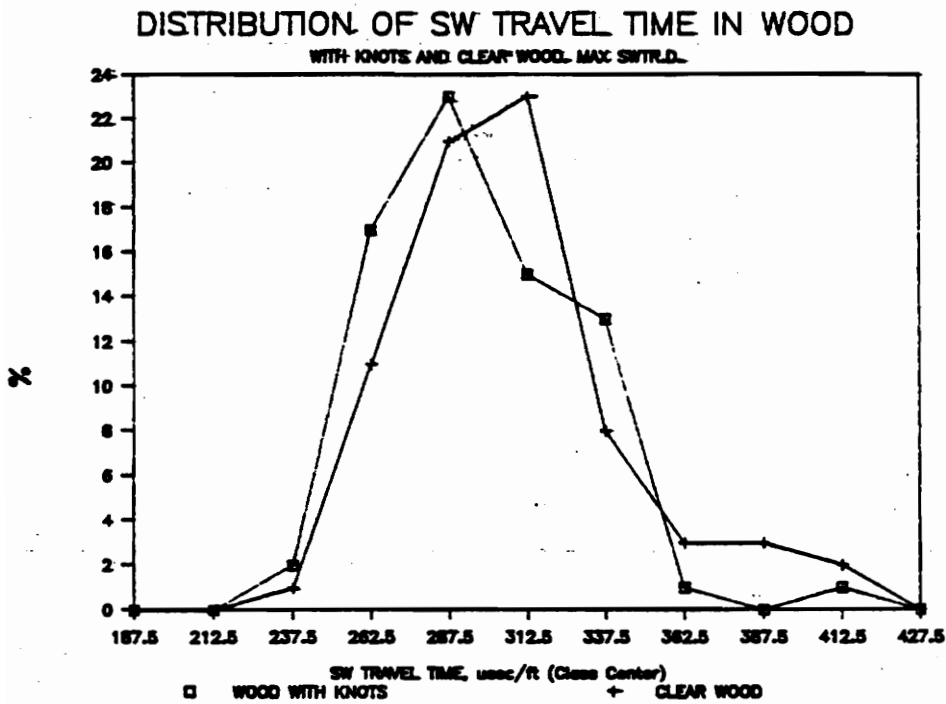
Appendix 4. (Continued)

2. Points with a Split, Check, Knot or Worm Hole:



Appendix 4. (Continued)

3. Points with a Knot:



Appendix 5. (Continued)

2. Possibly Mildly Infected Specimens

Stress Wave Travel Time

Stem Leaf	#	Boxplot
34 8	1	
33 02466	5	
32 335	3	
31 346	2	-----
30 235	3	-----
29 600	3	-----
28 1111124	7	-----
27 358999	6	-----
26 448	3	
25 358	2	

Multiply Stem Leaf by 10***1

Appendix 5. (Continued)

Maximum Tensile Stress

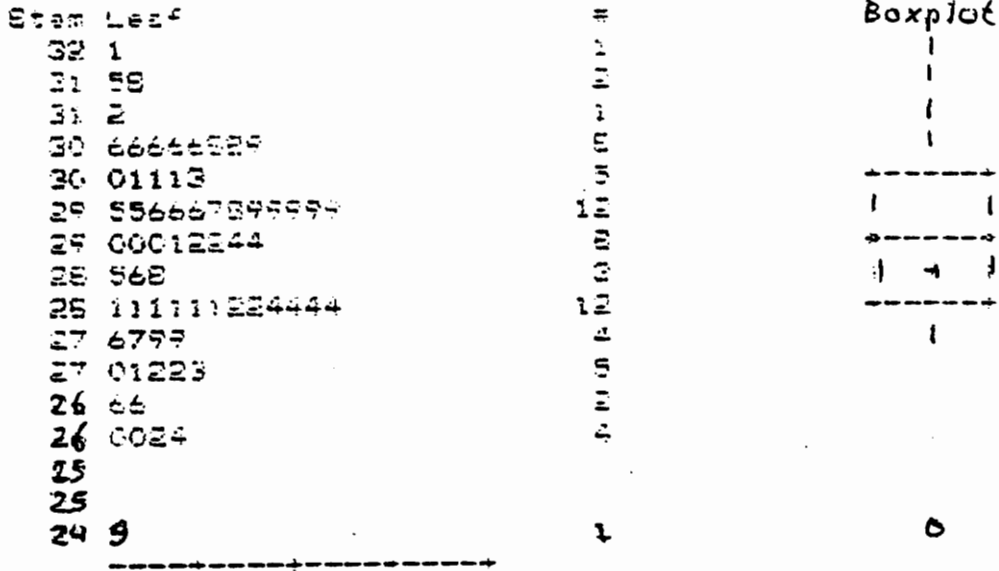
Stem Leaf	#	Boxplot
9 66	2	
9 02344	5	
8		
8 011223	6	-----
7 5566789	9	-----
7 0012	4	-
6 557789	9	-----
6		
5 6 8	3	
5 0 2	3	
4 4 7 8	4	0
3 3 4 5	5	0
3 0 2	3	0
2		
1		
1 3	1	*

-----+
 Multiply Stem Leaf by 10^{xx+2}

Appendix 5. (Continued)

3. Uninfected Specimens

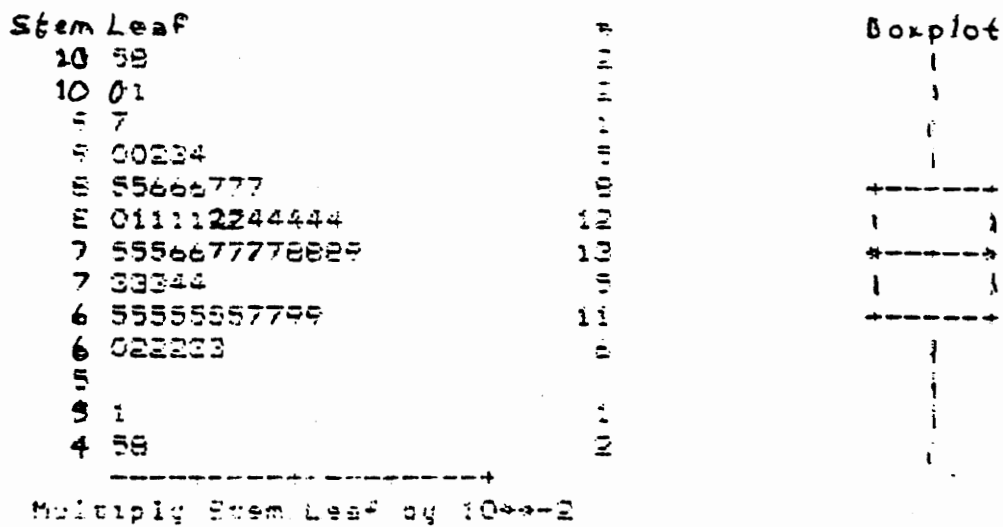
Stress Wave Travel Time



 Multiply Stem Leaf by 10^{stem+1}

Appendix 5. (Continued)

Maximum Tensile Stress



Appendix 6. (Continued)

2. Mixed Boards

Stem	Leaf	#	Boxplot
9	0	1	0
8			
8	00	2	0
7			
7			
6			
6	00	2	:
5			:
5			:
4			:
4	000000	6	:
3			:
3	000000000	9	+-----+
2			
2	0000000	7	
1			
1	000000000	9	
0	5555	4	+-----+
0	000000000000000000000000	23	
			+-----+

-----+-----+-----+-----+-----
 Multiply Stem. Leaf by 10**+1

Appendix 7. Tests on Stress Wave Travel Time at a Single
Analysis Point by Bacterial Infection Class.

Statistical Parameters for Flat-Sawn Material Only:

Bacterial Infection	N	x	Mn usec/ft	Std.Dev.	C.V. %
Certain	582	319	309	50.8	15.9
Possibly Mild	293	294	291	29.4	10.0
No	474	295	291	23.0	7.8
Total	1349	305	299	40.4	13.2

Kruskal-Wallis Tests:

Classes Between	Chi-Square	p
All	134.37	0.0001
Certainly Infected vs. Possibly Mildly Infected	79.490	0.0001
Certainly Infected vs. Uninfected	105.72	0.0001
Possibly Mildly Infected vs. Uninfected	0.01859	0.8915

Appendix 8. Tests on Stress Wave Travel Time in a Full-Size Board by Bacterial Infection Class.

Statistical Parameters for Flat-Sawn Boards Only:

Parameter	x	Mn	Std.Dev	C.V.	
Bacterial Infection		usec/ft		%	
—					
x					
Bacterial	84	316	315	33.9	10.7
Mixed	63	299	295	29.2	9.8
"Normal"	78	298	292	24.0	8.1
Total	225	305	302	30.5	10.0
Maximum					
Bacterial	84	362	333	80.3	22.1
Mixed	63	317	306	43.8	13.8
"Normal"	78	317	304	48.4	15.3
Total	225	334	315	64.8	19.4

Kruskal-Wallis Tests:

Classes Between Parameter	Stress Wave Travel Time			
	Chi-Square	Mean	Chi-Square	Maximum
		p		p
All	17.710	0.0001	26.402	0.0001
Bacterial Boards vs. Mixed Boards	11.584	0.0007	16.686	0.0001
Bacterial Boards vs. "Normal" Boards	13.594	0.0002	21.276	0.0001
Mixed Boards vs. "Normal" Boards	0.05393	0.8164	1.9531	0.1623

Appendix 9. Tests on Stress Wave Travel Time at a Point with a Defect and at an Adjacent Clear Point.

Statistical Parameters for and Sign and Sign Rank Tests on the Overall Effect of Defects to the Stress Wave Travel Time, usec/ft:

Statistical Parameter	Stress Wave Travel Distance			
	4-inch Point with Defect	4-inch Clear Point	Maximum Possible Point with Defect	Maximum Possible Clear Point
N	201	201	163	163
x	360	319	344	314
Mn	303	300	304	305
Std.Dev.	194	64	133	44.9
C.V., %	53.3	20.1	38.6	14.3
P				
Sign Test		0.7224		0.5764
Sign Rank Test		0.3612		0.3027

Statistical Parameters for and Paired t-tests on Stress Wave Travel Time, usec/ft, at a Point with a Particular Defect Compared to Adjacent Clear Wood:

Defect Statistical Parameter	Stress Wave Travel Distance			
	4-inch Point with Defect	4-inch Clear Point	Maximum Possible Point with Defect	Maximum Possible Clear Point
Splits				
N	22	22	18	18
x	838	429	652	348
Mn	824	418	627	341
Std.Dev.	553	154	357	56.2
C.V., %	66.0	35.9	54.8	16.1
t-obs		3.616		4.483
Significance		0.1 %		0.1 %

Appendix 9. (Continued)

Defect Statistical Parameter	Stress Wave Travel Distance			
	4-inch Point with Defect	Clear Point	Maximum Possible Point with Defect	Clear Point
Holes, Pith, Ring Failure				
<u>N</u>	93	93	73	73
x	310	306	315	311
Mn	300	297	305	310
Std.Dev.	37.2	29.8	53.6	47.2
C.V., %	12.0	9.7	17.0	15.2
t-obs	0.792		0.709	
Significance	50 %		50 %	
Knots				
<u>N</u>	86	86	72	72
x	292	306	297	309
Mn	289	300	293	306
Std.Dev.	29.3	35.2	33.9	37.0
C.V., %	10.0	11.5	11.4	12.0
t-obs	2.824		1.559	
Significance	1 %		20 %	

Appendix 9. (Continued)

Statistical Parameters for and Paired t-tests on the Effect of Defects to Stress Wave Travel Time at Certainly infected vs. Other Points:

Defect Bacterial Infection	Stress Wave Travel Distance			
	4-inch	Clear Point	Maximum Possible	Clear Point
Statistical Parameter	Point with Defect	Clear Point	Point with Defect	Clear Point
Splits				
Certain				
N	66	66	58	58
x	488	352	417	324
Mn	470	350	406	321
Std.Dev.	402	107	255	52.4
C.V., %	82.2	30.3	61.1	66.2
t-obs	2.671		2.701	
Significance	1 %		1 %	
Other				
N	49	49	33	33
x	307	300	320	307
Mn	302	296	297	297
Std.Dev.	42.6	25.7	63.5	47.5
C.V., %	13.9	8.6	19.8	15.5
t-obs	0.511		0.811	
Significance	-		50 %	
Knots				
Certain				
N	40	40	38	38
x	300	318	306	316
Mn	305	306	301	307
Std.Dev.	25.1	41.8	36.4	40.5
C.V., %	8.4	13.2	11.9	12.8
t-obs	2.337		1.128	
Significance	5 %		30 %	

Appendix 9. (Continued)

Defect Bacterial Infection	Stress Wave Travel Distance			
	4-inch	Maximum Possible		
Statistical Parameter	Point with Defect	Clear Point	Point with Defect	Clear Point
Knots				
Other				
N	46	46	34	34
x	285	296	288	301
Mn	288	293	278	289
Std.Dev.	31.3	24.5	28.7	31.4
C.V., %	11.0	8.3	9.9	10.4
t-obs		1.213		1.119
Significance		30 %		30 %

Appendix 10. Correlation and Stepwise Regression Analyses on
Stress Wave Travel Time in a Full-Size Board.

Correlation Analysis:

	Pearson Correlation Coefficients / Prob > R Under H : Rho = 0				
	SW2BMN	MAX2B	SAW	BUTT/TOP	INF
SW2BMN	1	0.91081	0.14255	-0.00939	-0.22910
	0	0.0001	0.0269	0.8847	0.0003
MAX2B	0.91081	1	0.19051	0.00200	-0.28164
	0.0001	0	0.0030	0.9754	0.0001
SAW	0.14255	0.19051	1	0.33543	-0.13469
	0.0269	0.0030	0	0.0001	0.0367
BUTT/TOP	-0.00939	0.00200	0.33543	1	-0.0580
	0.8847	0.9754	0.0001	0	0.3659
INF	-0.22910	-0.28164	-0.13469	-0.0580	1
	0.0003	0.0001	0.0367	0.3659	0
INF-%	0.23587	0.28802	-0.13468	0.00771	-0.98347
	0.0002	0.0001	0.0367	0.9052	0.0001
WIDTH	0.05172	0.01973	-0.03755	-0.11174	-0.04653
	0.4241	0.7606	0.5619	0.0634	0.4722
MC	0.22154	0.29717	0.05062	0.0392	-0.04173
	0.0005	0.0001	0.4350	0.5414	0.5200
GRDENS	-0.01499	0.08574	0.21522	0.05459	-0.08976
	0.8173	0.1856	0.0008	0.3999	0.1657
BSDENS	-0.16573	-0.13824	0.11407	0.02436	-0.03956
	0.0101	0.0323	0.0778	0.7073	0.5420

Appendix 10. (Continued)

	Pearson Correlation Coefficients /				
	Prob > !R! Under H : Rho = 0				
	INF-%	WIDTH	MC	GRDENS	BSDENS
SW2BMN	0.23587	0.05172	0.22154	-0.01499	-0.16573
	0.0002	0.4241	0.0005	0.8173	0.0101
MAX2B	0.28802	0.01973	0.29717	0.08754	-0.13824
	0.0001	0.7606	0.0001	0.1856	0.0323
SAW	0.13969	-0.03755	0.05062	0.21522	0.11407
	0.0302	0.5619	0.4350	0.0008	0.0778
BUTT/TOP	-0.00501	-0.11174	0.03962	0.05459	0.02436
	0.9383	0.0834	0.5414	0.3999	0.7073
INF	-0.98347	-0.04653	-0.04173	-0.08976	-0.03956
	0.0001	0.4722	0.5200	0.1657	0.5420
INF-%	1	0.05167	0.03191	0.08590	0.04385
	0	0.4246	0.6228	0.1848	0.4990
WIDTH	0.05167	1	0.04279	0.00325	-0.02727
	0.4246	0	0.5094	0.9601	0.6743
MC	0.03191	0.04279	1	0.06862	-0.68448
	0.6228	0.5094	0	0.2897	0.0001
GRDENS	0.08590	0.00325	0.06862	1	0.66883
	0.1848	0.9601	0.2897	0	0.0001
BSDENS	0.04385	-0.02727	-0.68448	0.66883	1
	0.4990	0.6743	0.0001	0.0001	0

Appendix 10. (Continued)

Summaries of Stepwise Procedures:

For Dependent Variable SW2BMN

Step	Variable Entered	Partial R-Square	Model R-Square	C(p)	F	Prob>F
1	INF-%	0.0554	0.0554	13.4588	13.9562	0.0002
2	MC	0.0459	0.1012	3.3491	12.0919	0.0006
3	SAW	0.0102	0.1114	2.6568	2.7077	0.1012

For Dependent Variable SW2BMN

Step	Variable Entered	Partial R-Square	Model R-Square	C(p)	F	Prob>F
1	MC	0.0883	0.0883	30.9555	23.0534	0.0001
2	INF-%	0.0773	0.1656	10.3280	21.9489	0.0001
3	SAW	0.0192	0.1848	6.6991	5.5652	0.0191

List of Variables:

- SW2BMN = Mean Stress Wave Travel Time, Maximum Possible Travel Distance, Clear Points Only.
- MAX2B = Maximum Stress Wave Travel Time, Maximum Possible Travel Distance, Clear Points Only.
- SAW = Grain Pattern Class.
- BUTT/TOP = Location of Board in a 12-foot Log.
- INF = Bacterial Infection Class.
- INF-% = Percentage Bacterially Infected Volume.
- WIDTH = Board Width.
- MC = Average Moisture Content by Samples from Butt and Top End.
- GREDENS = Average Green Density by Samples from Butt and Top End.
- BSDENS = Average Basic Density by Samples from Butt and Top End.

Appendix 11. Tests on Tensile Strength Perpendicular to Grain by Bacterial Infection Class.

Statistical Parameters:

Variable	N	x	Mn	Std.Dev.	C.V. %
Bacterial Infection					
Stress Wave Travel Time, usec/ft					
Certain	139	338	314	63.3	18.7
Possibly Mild	37	295	284	26.2	8.9
No	68	289	291	15.3	5.3
Maximum Tensile Stress, psi					
Certain	139	440	471	285	64.7
Possibly Mild	37	711	752	196	27.5
No	68	772	775	126	16.3

Kruskal-Wallis Tests:

Classes Between Variable	Chi-Square	p
All		
Stress Wave Travel Time	71.907	0.0001
Maximum Tensile Stress	75.825	0.0001
Certainly vs. Possibly Mildly Infected Specimens		
Stress Wave Travel Time	22.857	0.0001
Maximum Tensile Stress	28.816	0.0001
Certainly Infected vs. Uninfected Specimens		
Stress Wave Travel Time	65.543	0.0001
Maximum Tensile Stress	64.134	0.0001
Possibly Mildly Infected vs. Uninfected Specimens		
Stress Wave Travel Time	0.154	0.6970
Maximum Tensile Stress	1.315	0.2514

Appendix 12. Correlation and Stepwise Regression Analyses on
Tensile Strength Perpendicular to Grain.

Correlation Analysis:

Pearson Correlation Coefficients / Prob > !R! Under H : Rho = 0					
	MAXSTR	SWTMAX	MC	GRDENS	BSDENS
MAXSTR	1	-0.72426	-0.29702	-0.11216	0.13539
	0	0.0001	0.0269	0.0804	0.0345
SWTMAX	0.72426	1	0.30544	0.14625	-0.14001
	0.0001	0	0.0001	0.0223	0.0287
MC	-0.29702	0.30544	1	0.04933	-0.71643
	0.0001	0.0001	0	0.4431	0.0001
GRDENS	-0.11216	0.14625	0.04933	1	0.58925
	0.0804	0.0223	0.4431	0	0.0001
BSDENS	0.13539	-0.14001	-0.71643	-0.58925	1
	0.0345	0.0287	0.0001	0.0001	0
INF	0.53199	-0.40489	-0.33671	-0.23141	0.10144
	0.0001	0.0001	0.0001	0.0003	0.1140
FAILURE	-0.11844	0.02176	-0.06560	-0.09493	-0.00638
	0.0647	0.7352	0.3075	0.1392	0.9211

Pearson Correlation Coefficients / Prob > !R! Under H : Rho = 0		
	INF	FAILURE
MAXSTR	0.53199	-0.11844
	0.0001	0.0647
SWTMAX	-0.40489	0.02176
	0.0001	0.7352
MC	-0.33671	-0.06560
	0.0001	0.3075
GRDENS	-0.23141	-0.09493
	0.0003	0.1392
BSDENS	0.10144	-0.00638
	0.1140	0.9211
INF	1	-0.01921
	0	0.7653
FAILURE	-0.01921	1
	0.7653	0

Appendix 12. (Continued)

Summary of Stepwise Procedure for Dependent Variable MAXSTR:

Step	Variable Entered	Partial R-Square	Model R-Square	C(p)	F	Prob>F
1	SWTMAX	0.5871	0.5871	64.8954	344.123	0.0001
2	GRDENS	0.0578	0.6450	24.1863	39.258	0.0001
3	INF	0.0227	0.6677	9.3864	16.4311	0.0001
4	BSDENS	0.0098	0.6774	6.2077	2.4037	0.1224

List of Variables:

MAXSTR = Maximum Tensile Stress.
 SWTMAX = Stress Wave Travel Time, Maximum Possible Travel Distance.
 MC = Moisture Content.
 GRDENS = Green Density.
 BSDENS = Basic Density.
 INF = Bacterial Infection Class.
 FAILURE = Failure Pattern Class.

Appendix 13. Tests on Drying Defects at a Single Stress Wave
Analysis Point by Bacterial Infection Class.

Defects in Flat-Sawn Material Only:

<u>Bacterial Infection</u>					
	N	Light	Honeycomb		Total Observed
			Medium	Heavy	
			%		
Certain	374	1.6	8.9	6.0	16.5
Possibly Mild	249	0.8	1.9	2.7	5.3
No	368	1.5	4.8	1.3	7.5
Total	991	1.4	5.8	3.5	10.6

	N	Light	Surface Checks		Total Observed
			Medium	Heavy	
			%		
Certain	374	2.2	9.2	2.7	14.0
Possibly Mild	249	1.9	3.4	1.1	6.5
No	368	1.5	4.3	1.8	7.5
Total	991	1.9	6.0	2.0	9.9

	N	Ring Failure			Total Observed
		Single Near Surface	Single Throughout	Multiple	
		%			
Certain	374	7.4	9.8	10.0	27.2
Possibly mild	249	4.2	2.7	1.5	9.1
No	368	4.3	2.0	1.8	8.0
Total	991	5.6	5.3	5.1	16.2

	N	Light	Any Defect		Total Observed
			Medium	Heavy	
			%		
Certain	405	11.5	16.8	11.5	39.9
Possibly Mild	266	10.6	6.8	4.4	21.8
No	372	9.3	7.2	3.6	20.0
Total	1043	10.5	11.3	7.2	29.0

Appendix 13. (Continued)

Chi-Square Tests:

	Chi-Square	p
Honeycomb	51.219	0.000
Surface Checks	37.801	0.000
Ring Failure	96.010	0.000
Any Defect	59.133	0.000

Appendix 14. Tests on Drying Defects in a Full-Size, Flat-Sawn Board by Bacterial Infection Class.

Bacterial Infection						
	N	Light	Honeycomb Medium	Heavy	Total Observed	
			%			
Bacterial	63	4.8	25.4	19.1	49.2	
Mixed	58	5.2	13.8	10.3	29.3	
"Normal"	64	3.1	12.5	7.8	23.4	
Total	185	4.3	17.3	12.4	34.0	

Surface checks						
	N	Light	Medium	Heavy	Total Observed	
			%			
Bacterial	63	9.5	22.2	11.1	42.9	
Mixed	58	6.9	19.0	3.5	29.3	
"Normal"	64	4.7	14.1	7.8	26.6	
Total	185	7.0	18.4	7.6	33.0	

Ring Failure						
	N	Single Near Surface	Single Throughout	Multiple	Total Observed	
			%			
Bacterial	63	11.1	14.3	31.8	57.1	
Mixed	58	10.3	10.3	8.6	29.3	
"Normal"	64	9.4	4.7	6.3	20.3	
Total	185	10.3	9.7	15.7	35.7	

Appendix 14. (Continued)

<u>Bacterial Infection</u>				
	N	End Checks and Splits		Total Observed
		Butt	Top	
		%		
Bacterial	63	34.9	9.5	41.1
Mixed	58	17.3	10.3	25.2
"Normal"	64	17.2	9.3	24.8
Total	185	23.2	9.7	30.5

	N	Any Defect			Total Observed
		Light	Medium	Heavy	
		%			
Bacterial	63	12.7	30.2	44.4	87.3
Mixed	58	12.1	27.6	17.2	56.9
Normal	64	17.2	17.2	15.6	50.0
Total	185	14.1	24.9	26.0	64.9

Chi-Square Tests:

Defect	Chi-Square	p
Honeycomb	10.234	0.006
Surface Checks	4.327	0.115
Ring Failure	20.258	0.000
End Splits	23.800	0.041
Any Defect	21.737	0.000

Appendix 15. Tests on Drying Defects at a Single Stress Wave Analysis Point by Stress Wave Travel Time Class.

Stress Wave Travel Time, usec/ft					
	N	Light	Honeycomb		Total Observed
			Medium	Heavy	
			%		
> 350	59	3.0	22.6	18.9	44.5
280-350	725	2.1	4.5	1.4	8.0
< 280	325	1.5	5.6	1.4	7.5
Surface Checks					
	N	Light	Medium	Heavy	Total Observed
			%		
> 350	59	1.1	6.9	13.6	21.6
280-350	725	2.3	5.7	1.3	9.3
< 280	325	2.1	3.3	0.3	5.7
Ring Failure					
	N	Single Near Surface	Single Throughout	Multiple	Total Observed
		%			
> 350	59	2.2	12.1	31.3	45.5
280-350	725	7.2	6.5	3.1	16.8
< 280	325	2.5	2.8	1.0	6.2
Any Defect					
	N	Light	Medium	Heavy	Total Observed
		%			
> 350	59	5.3	19.2	37.5	62.0
280-350	725	12.0	6.6	2.3	20.9
< 280	325	10.1	6.0	0.7	16.8

Appendix 15. (Continued)

Chi-Square Tests:

Defect	Chi-Square	p
Honeycomb	78.503	0.000
Surface Checks	14.299	0.000
Ring Failure	54.601	0.000
Any Defect	81.581	0.000

Appendix 16. Tests on Drying Defects in a Full-Size, Flat Sawn Board by the Class of Maximum Stress Wave Travel Time Observed.

Maximum Stress Wave Travel Time Observed, usec/ft						
	N	Light	Honeycomb		Heavy	Total Observed
			Medium			
			%			
> 350	35	5.7	31.4		40.0	77.1
280-350	131	4.6	13.0		6.9	24.4
< 280	19	0.0	21.0		0.0	21.0
Surface Checks						
	N	Light	Medium	Heavy		Total Observed
			%			
> 350	35	0.0	22.9		22.9	45.7
280-350	131	8.4	19.9		4.6	32.8
< 280	19	10.5	0.0		0.0	10.5
Ring Failure						
	N	Single Near Surface	Single Throughout	Multiple		Total Observed
		%				
> 350	35	14.3	14.3		48.6	77.1
280-350	131	9.9	9.9		9.2	29.0
< 280	19	5.3	0.0		0.0	5.3

Appendix 16. (Continued)

Maximum Stress Wave Travel Time Observed, usec/ft				
	N	End Checks and Splits		Total Observed
		Butt	Top	
		%		
> 350	35	66.7	19.0	72.0
280-350	131	11.7	7.8	14.1
< 280	19	0.0	0.0	0.0

	N	Any Defect			Total Observed
		Light	Medium	Heavy	
		%			
> 350	35	2.9	22.9	65.7	91.4
280-350	131	15.3	26.0	19.1	60.3
< 280	19	26.3	21.1	0.0	47.4

Chi-Square Tests:

Defect	Chi-Square	p
Honeycomb	38.576	0.000
Surface Checks	10.671	0.005
Ring Failure	44.321	0.000
End Splits	65.302	0.000
Any Defect	49.117	0.000

Appendix 17. Correlation and Stepwise Regression Analyses on
Percentage Degraded Board Volume.

Correlation Analysis:

Pearson Correlation Coefficients /					
Prob > R Under H : Rho = 0					
	DEGRADE	SW2BMN	MAX2B	BUTT/TOP	SAW
DEGRADE	1	0.45188	0.49140	-0.00952	0.27177
	0	0.0001	0.0001	0.8933	0.0001
SW2BMN	0.45188	1	0.91635	0.01020	0.18166
	0.0001	0	0.0001	0.8857	0.0099
MAX2B	0.49140	0.91635	1	0.03184	0.25625
	0.0001	0.0001	0	0.6537	0.0003
BUTT/TOP	-0.00952	0.01020	0.03184	1	0.30201
	0.8933	0.8857	0.6537	0	0.0001
SAW	0.27177	0.18166	0.25625	0.30201	1
	0.0001	0.0099	0.0003	0.0001	0
INF	-0.39299	0.19278	-0.24352	0.01564	-0.18016
	0.0001	0.0061	0.0005	0.8256	0.0105
INF-%	0.36821	0.19205	0.24309	-0.00319	-0.18852
	0.0001	0.0063	0.0005	0.9642	0.0074
WIDTH	0.22484	0.08061	0.04093	-0.07105	0.01463
	0.0013	0.2553	0.5640	0.3162	0.8367
MC	0.22293	0.18778	0.25716	0.02622	0.05009
	0.0015	0.0076	0.0002	0.7118	0.4801
GRDENS	0.07208	-0.02994	0.06572	0.04389	0.22703
	0.3092	0.6731	0.3540	0.5361	0.0012
BSDENS	-0.11845	-0.16411	-0.14370	0.03327	0.12558
	0.0940	0.0199	0.0418	0.6392	0.0757

Appendix 17. (Continued)

	Pearson Correlation Coefficients /				
	Prob > R Under H : Rho = 0				
	INF	INF-%	WIDTH	MC	GRDENS
DEGRADE	-0.39299 0.0001	0.36281 0.0001	0.22484 0.0013	0.22293 0.0015	0.07208 0.3092
SW2BMN	-0.19278 0.0061	0.19205 0.0063	0.08061 0.2553	0.18778 0.0076	-0.02994 0.6731
MAX2B	-0.24352 0.0005	0.24309 0.0005	0.04093 0.5640	0.25716 0.0002	0.06572 0.3540
BUTT/TOP	0.01564 0.8256	-0.00319 0.9445	-0.07105 0.3162	0.02622 0.7118	0.04389 0.5361
SAW	-0.18016 0.0001	0.18852 0.0099	0.01463 0.0003	0.05009 0.0001	0.22703 0.0012
INF	1 0	-0.98334 0.0001	-0.10927 0.1226	-0.00030 0.9926	-0.07616 0.2825
INF-%	-0.98334 0.0001	1 0	0.11107 0.1226	-0.01557 0.9966	0.06728 0.2825
WIDTH	-0.10927 0.1226	0.11107 0.1165	1 0	0.05775 0.4155	0.01072 0.8300
MC	-0.00030 0.9966	-0.01557 0.8264	0.05775 0.4155	1 0	0.06265 0.3769
GRDENS	-0.07616 0.2825	0.06728 0.3426	0.01072 0.8800	0.06265 0.3769	1 0
BSDENS	-0.05279 0.4567	0.05831 0.4110	-0.03336 0.6383	-0.68952 0.0001	0.67631 0.0001

Appendix 17. (Continued)

Pearson Correlation Coefficients / Prob > R Under H : Rho = 0	
	BSDENS
DEGRADE	-0.11840
	0.0940
SW2BMN	-0.16411
	0.0199
MAX2B	0.14370
	0.0418
BUTT/TOP	0.03322
	0.6592
SAW	0.12558
	0.0757
INF	-0.05279
	0.4567
INF-%	0.05831
	0.4110
WIDTH	-0.0336
	0.6383
MC	-0.68952
	0.0001
GRDENS	0.6731
	0.0001
BSDENS	1
	0

Appendix 17. (Continued)

Summary of Stepwise Procedure for Dependent Variable
DEGRADE:

Step	Variable Entered	Partial R-Square	Model R-Square	C(p)	F	Prob>F
1	MAX2B	0.2922	0.2922	49.2847	82.1725	0.0001
2	SAW	0.0288	0.3843	21.2571	9.2044	0.0027
3	WIDTH	0.0212	0.4054	15.8965	6.9730	0.0089
4	INF-%	0.0112	0.4167	13.9890	3.7537	0.0541
5	GRDENS	0.0147	0.4314	12.6115	3.2826	0.0716
6	BSDENS	0.0122	0.4440	10.4760	3.1919	0.0756

List of Variables:

DEGRADE = Percentage of Degraded Volume of a Board.
 SW2BMN = Mean Stress Wave Travel Time, Maximum Possible Travel Distance, Clear Points Only.
 MAX2B = Maximum Stress Wave Travel Time, Maximum Possible Travel Distance, Clear Points Only.
 BUTT/TOP = Location of Board in a 12-Foot Log.
 SAW = Grain Pattern Class.
 INF = Bacterial Infection Class.
 INF-% = Percentage Bacterially Infected Volume.
 WIDTH = Board Width.
 MC = Average Moisture Content by Samples from Butt and Top End.
 GRDENS = Average Green Density by Samples from Butt and Top End.
 BSDENS = Average Basic Density by Samples from Butt and Top End.

VITA

The author was born in Vihanti, Finland, on December 14, 1959. He received a degree of Master of Science in Agriculture and Forestry from the University of Helsinki, Finland, in November of 1984, with Forest Engineering as his major subject. Since his graduation, the author is employed as a researcher in wood utilization by the Finnish Forest Research Institute, Department of Forest Technology.

The author entered the graduate program of Wood Science and Forest Products at Virginia Tech in August of 1990 and graduated with a Master of Science in Forestry and Forest Products in December of 1991, under the direction of Prof. Robert L. Youngs. After his graduation, the author will continue his research work in the Finnish Forest Research Institute.

Erkki Ilmari Verkasalo

Erkki Ilmari Verkasalo